

TR 84035

BR93481
TR 84035

③

UNLIMITED



ROYAL AIRCRAFT ESTABLISHMENT

Technical Report 84035

April 1984

THE EFFECT OF FRICTIONAL FORCES ON FATIGUE CRACK GROWTH IN LUGS

by

J. E. Moon

DTIC
ELECTE
MAR 27 1985
S E D

DTIC FILE COPY

Procurement Executive, Ministry of Defence
Farnborough, Hants

UNLIMITED

UNLIMITED

UDC 621.886.4 : 539.219.2 : 539.431 : 539.211 : 539.4.014.11 : 531.4

ROYAL AIRCRAFT ESTABLISHMENT

Technical Report 84035

Received for printing 4 April 1984

THE EFFECT OF FRICTIONAL FORCES ON FATIGUE CRACK GROWTH IN LUGS

by

J. E. Moon

SUMMARY

↙ In a previous Report by the author, experimental stress intensity factor range ~~and~~ distributions derived from crack propagation rate measurements were presented for a pin-loaded lug. It was shown that crack growth rate at short crack lengths was much faster, by up to almost an order of magnitude, than predicted by available fracture mechanics solutions. It was proposed that this was due to the action of frictional forces between the pin and hole surface. These forces are normally ignored, it being assumed that load is transferred by radial pressure alone.

Further crack propagation rate measurements have been made on lugs with normal clearance fit pins which confirm the earlier results.

Experiments are described in which the frictional forces were reduced by lubricant and removed altogether from around the crack origin using pins with flats. It is found that crack propagation rate at short crack lengths is significantly reduced by both of these measures, indicating values of ΔK nearer to those predicted ignoring frictional forces.

↖ It is found that the inclusion of the action of frictional forces in a fracture mechanics analysis of a lug leads to an increase in the predicted ΔK at short crack lengths. Closer agreement with experimental results is obtained if it is assumed that these forces build up more in the region of the crack origin and are therefore effective for the important region of short crack lengths. ↗

Departmental Reference: Materials/Structures 79

Copyright

©
Controller HMSO London
1984

The substance of this Report was presented at the 12th Symposium of the International Committee on Aeronautical Fatigue, held at Toulouse, France, 25-27 May 1983.

LIST OF CONTENTS

UNLIMITED

	<u>Page</u>
1 INTRODUCTION	3
2 EXPERIMENTAL STRESS INTENSITY FACTOR DISTRIBUTIONS	3
2.1 Specimens and materials	3
2.2 Experimental procedure and method of analysis	4
2.3 Discussion of crack propagation test results	5
2.3.1 Clearance fit pin with no lubricant	5
2.3.2 Lubricated pins	5
2.3.3 Pins with flats	6
2.3.4 Comparison of behaviour of three cases tested	6
3 MECHANISM OF LOAD TRANSFER BETWEEN PIN AND LUG	7
4 THEORETICAL PREDICTIONS OF CRACK PROPAGATION IN A LUG	10
4.1 Pins with flats	10
4.2 Clearance fit pin with lubricant	10
4.3 Clearance fit pin without lubricant	11
4.4 Sensitivity of prediction to assumed distribution of frictional forces	15
5 CONCLUDING REMARKS	16
Appendix Load transfer by radial pressure and frictional forces	19
List of symbols	23
References	24
Illustrations	Figures 1-24
Report documentation page	inside back cover

Accession For	
NTIS GRA&I	<input checked="" type="checkbox"/>
DTIC TAB	<input type="checkbox"/>
Unannounced	<input type="checkbox"/>
Justification	
By	
Distribution/	
Availability Codes	
Dist	Avail and/or Special
A-11	

1 INTRODUCTION

In a previous Report¹, the author presented experimental stress intensity factor range (ΔK) distributions derived from crack propagation rate measurements, for the case of a pin loaded lug. It was shown that ΔK at relatively short crack lengths was higher than predicted by available fracture mechanics solutions. It was suggested that this effect was due to the omission of the effects of frictional forces between the pin and hole surface in theoretical analyses of crack growth behaviour. Studies of fretting fatigue using plain specimens with fretting pads have shown that relative slip between two surfaces leads to the build up of frictional forces and that these forces can cause a significant increase in crack growth rate at short crack lengths^{2,3}.

The results are presented in this Report of the subsequent work which has been carried out investigating the action of frictional forces in lugs in order to understand the observed crack growth behaviour.

Crack growth measurement experiments have been carried out on lugs in which the frictional forces around the crack origin were reduced or removed altogether. The results, which are presented in section 2, allow an assessment to be made of the magnitude of the effect of frictional forces on crack growth rate.

It is found that the reduction of frictional forces by the introduction of a lubricant between the pin and hole surface leads to a reduction in crack growth rate at short crack lengths. The removal of these forces altogether from the area of the crack origin, by the use of a pin with flats machined on, leads to an even greater reduction in growth rate. It is concluded that the presence of frictional forces in a lug with a normal dry assembled clearance fit pin is sufficient to cause the high crack growth rates observed¹. Therefore, in order to predict accurately the rate of crack growth, these frictional forces must be included in the model for the analysis. In order to do this, the magnitude and distribution of radial pressure and frictional forces must be known. The derivation of an estimate of these distributions, from work described previously¹, is described in section 3.

Presented in section 4 are the results of including the action of frictional forces in a fracture mechanics analysis, to see if the observed trends can be predicted, in a similar manner to the predictions of Edwards and Cook² for the case of plain specimens with fretting pads. Sensitivity of the result to the nature of the assumption is then checked in order to identify the important parameters which control the growth of a crack in a lug. It is found that the effects of using normal pins with and without lubricant and pins with flats on the rate of growth of cracks can be predicted well. The actual magnitude of the frictional forces close to the crack origin are found to be very important, governing the growth of small cracks.

2 EXPERIMENTAL STRESS INTENSITY FACTOR DISTRIBUTIONS

2.1 Specimens and materials

The lug used in this series of experiments is shown in Fig 1. It can be seen that it is relatively thick ($(\text{thickness } (t)/\text{diameter } (d)) = 0.94$), which leads to crack

initiation taking place near the corners at the minimum section due to pin bending^{4,5}. Generally, fatigue cracks started propagating as a semi-ellipse from an initiation point about 1 mm from the corner along the bore. They quickly became quarter-elliptical on breaking through to the surface and remained in this form for most of the remaining life.

The specimens were manufactured as a single batch from the same melt of BS2L65 aluminium alloy material.

The lugs were assembled in three conditions:

- (a) Some of the lugs were assembled with degreased clearance (0.03-0.21%) fit steel pins. This is the same condition as tested and reported previously¹ and was used in order to confirm the results obtained.
- (b) Several lugs were assembled with a water displacing penetrant/lubricant, replenished at regular intervals throughout the test without dismantling the assembly. Studies of fretting fatigue using aluminium alloy plain specimens with steel fretting pads have shown that frictional forces can be reduced significantly by such a compound⁶.
- (c) The third batch of lugs was assembled using pins with flats, as shown in the inset to Fig 1. A pin flat angle of 60° was chosen to give a significant improvement in fatigue strength, as described in a review of methods of improving the fatigue performance of lugs⁷. With such pins, failure took place in the unfretted region of the hole at the minimum section, ie in approximately the same location as in lugs assembled using normal pins with and without lubricant, conditions (a) and (b) above. Thus, there were no radial or shear forces within a 60° arc on either side of the crack origin.

2.2 Experimental procedure and method of analysis

Measurements of crack propagation rate in the lugs were made by post-failure fracture surface analysis. The procedure adopted has been described in detail previously¹, and will therefore only be outlined here. The specimens were subjected to a repeating two level high-low block programme loading sequence shown schematically on Fig 2. The repeating block of several thousand 'low level' cycles marked the fracture surface with a series of fine lines, as shown in the photomicrograph of Fig 3. Measurement of the distance between the marker lines, using an optical microscope, allowed direct determination of the crack propagation rate at the higher load level by dividing this distance by the number of cycles in the block. The crack length pertaining to this rate was taken to be mid-way between the marker lines. The number of cycles in each block and stress levels were adjusted as necessary for each assembly condition to achieve a finely marked fracture surface giving good resolution at short crack lengths. The stress level at which measurements were required (the high level in the repeating sequence) was the same for the two cases of normal pins with and without lubricant, but had to be increased in the tests using pins with flats in order to promote failure in a similar number of cycles.

initiation taking place near the corners at the minimum section due to pin bending^{4,5}. Generally, fatigue cracks started propagating as a semi-ellipse from an initiation point about 1 mm from the corner along the bore. They quickly became quarter-elliptical on breaking through to the surface and remained in this form for most of the remaining life.

The specimens were manufactured as a single batch from the same melt of BS2L65 aluminium alloy material.

The lugs were assembled in three conditions:

- (a) Some of the lugs were assembled with degreased clearance (0.03-0.21%) fit steel pins. This is the same condition as tested and reported previously¹ and was used in order to confirm the results obtained.
- (b) Several lugs were assembled with a water displacing penetrant/lubricant, replenished at regular intervals throughout the test without dismantling the assembly. Studies of fretting fatigue using aluminium alloy plain specimens with steel fretting pads have shown that frictional forces can be reduced significantly by such a compound⁶.
- (c) The third batch of lugs was assembled using pins with flats, as shown in the inset to Fig 1. A pin flat angle of 60° was chosen to give a significant improvement in fatigue strength, as described in a review of methods of improving the fatigue performance of lugs⁷. With such pins, failure took place in the unfretted region of the hole at the minimum section, ie in approximately the same location as in lugs assembled using normal pins with and without lubricant, conditions (a) and (b) above. Thus, there were no radial or shear forces within a 60° arc on either side of the crack origin.

2.2 Experimental procedure and method of analysis

Measurements of crack propagation rate in the lugs were made by post-failure fracture surface analysis. The procedure adopted has been described in detail previously¹, and will therefore only be outlined here. The specimens were subjected to a repeating two level high-low block programme loading sequence shown schematically on Fig 2. The repeating block of several thousand 'low level' cycles marked the fracture surface with a series of fine lines, as shown in the photomicrograph of Fig 3. Measurement of the distance between the marker lines, using an optical microscope, allowed direct determination of the crack propagation rate at the higher load level by dividing this distance by the number of cycles in the block. The crack length pertaining to this rate was taken to be mid-way between the marker lines. The number of cycles in each block and stress levels were adjusted as necessary for each assembly condition to achieve a finely marked fracture surface giving good resolution at short crack lengths. The stress level at which measurements were required (the high level in the repeating sequence) was the same for the two cases of normal pins with and without lubricant, but had to be increased in the tests using pins with flats in order to promote failure in a similar number of cycles.

Values of ΔK were obtained from the crack propagation rate measurements using materials data of ΔK vs crack propagation rate obtained on specimens for which an accurate stress intensity factor solution was available. As in the previous work¹, the data for BS2L65 material was taken from Ref 8, which used Refs 9 and 10 as its sources. As discussed previously¹, Pearson's data¹¹, for R (= minimum stress/maximum stress) = 0 loading, obtained on thicker specimens (12.7 mm instead of 5 mm), suggests that the data used may produce values of ΔK at a particular growth rate between 10-20% too high in the range under consideration. This point will be referred to later. In order to allow easier, direct comparison the ΔK values were normalised to obtain the correction function Y by dividing by K_0 ($= \sigma \sqrt{\pi a}$); where σ_g is the alternating gross section stress.

A crack propagation rate vs crack length (a) graph for one example of a lug with a normal dry clearance fit pin is plotted on Fig 4 and for a lug loaded by a lubricated pin in Fig 5. The corresponding graph for all three lugs tested using pins with flats is presented in Fig 6. The desired values of Y for all specimens are plotted against relative crack length (a/r) on Figs 7 to 9 for the cases of normal dry pins, lubricated pins and pins with flats respectively. Mean lines were drawn by eye through the data, as shown on these Figures, and these lines are compared on Fig 10. The only case for which drawing a mean line was difficult was that for lubricated pins at short crack lengths; this point will be referred to in the next section.

2.3 Discussion of crack propagation test results

2.3.1 Clearance fit pin with no lubricant

As stated earlier, this is the pin condition for which results were presented and discussed in detail previously¹. At that time only two results for lugs of BS2L65 material were available. The results for three further specimens can now be compared with the original data. The derived values of Y for all specimens are plotted on Fig 7. It can be seen that there is very little scatter in the results, the later results confirming those already presented, in particular the high values of Y at short crack lengths.

2.3.2 Lubricated pins

The results for clearance fit pins with no lubricant indicated that the low level marker loads were hardly damaging, the number of cycles up to failure at the higher level comparing reasonably well with the log mean life achieved in normal constant amplitude fatigue tests at that loading level¹². Thus, the comparison of lives at the higher level for the lubricated pin tests with the results from normal fatigue tests using dry, unlubricated pins should give a reliable measure of the beneficial effect on life of using the lubricant. The results indicate that the use of lubricant leads to an increase in endurance by a factor of approximately 2.6.

Turning now to the crack growth rate measurements, a lot of scatter was observed in the results of the four specimens for crack lengths less than 2 mm. Growth tended to be erratic. This was probably due to the difficulty in maintaining fresh lubricant on the pin at all times. As the lubricant becomes less effective and migrates away from the

area of the crack origin, the frictional forces would be allowed to build up. The results derived from all four specimens are presented on Fig 8 which plots the values of Y against relative crack length a/r . It was assumed that the lug which exhibited the generally lower crack rates at short crack lengths was the one in which the most success was achieved in keeping fresh lubricant on the pin during this phase of life. Therefore the mean curve was drawn through the results for this particular lug for $a/r < 0.15$. The crack growth rate measurements for this lug are presented in Fig 5. This graph shows that after some slightly erratic behaviour for crack lengths less than 0.5 mm, growth rate increased fairly steadily to reach a peak at around 2 mm. The crack then slowed down over the next 1 mm to reach a rate which remained fairly constant up to 7 mm.

Comparison with the result obtained using a dry pin (Fig 4) shows that growth rate was significantly lower at all points. This is reflected in Fig 10 which compares values of Y against a/r for the three experimental cases.

2.3.3 Pins with flats

These crack propagation tests had to be carried out at an alternating stress level which was approximately twice that employed in the tests using normal pins with and without lubricant. This was due to the large increase in fatigue strength which can be achieved using such pins⁷. The increased stress level meant that the tests were conducted in a region where changes in fretting damage would be expected to be less effective. However, the results indicate a life improvement factor due to the use of pins with flats of between 8 and 25.

The low number of rate measurements made on each specimen allowed the results for all three specimens to be plotted on Fig 6. When viewing this graph, it must be remembered that the applied stress levels were considerably higher than in the tests using normal pins. This would not be expected to affect the derived Y distributions although the growth rates were higher. It is obvious that the form of the curve is very different from the other two cases in that crack growth rate increased fairly steadily to failure, there being no peak or period of constant growth rate.

The scatter in crack propagation behaviour for the three cases can be assessed by comparing Figs 7, 8 and 9 which present the derived values of Y against a/r for all specimens tested. It can be seen that the use of pins with flats led to less scatter in crack growth at short crack lengths than the lubricated pins. However, at crack lengths above 3-4 mm the pins with flats led to the greatest scatter in results of all three experimental cases. Nevertheless, the experimental repeatability appears to be adequate.

2.3.4 Comparison of behaviour of three cases tested

The mean curves of Y vs a/r for all three experimental cases are compared on Fig 10. As Y is non-dimensional, the fact that different stress levels were applied in the tests is removed.

It is immediately apparent that the very high values of Y observed for a lug loaded by a normal dry pin were not produced by the cases of lubricated pins or pins with flats. The reduction of frictional forces by the introduction of lubricant led to a

sharp fall in Y for $a/r < 0.1$, and the removal of all frictional and radial forces from a large area around the crack origin led to an even larger fall in Y for the case of pins with flats.

The effect may be visualised better by examining Fig 11 which compares crack growth rates for the three cases at the same stress level. This Figure was constructed using the mean Y curves of Fig 10, going in the reverse order through the procedure described in section 2.2 for deriving Y values from crack growth rate measurements. Also plotted on Fig 11 is the predicted crack growth behaviour using Newman's solution¹³, which was used as a comparison previously¹. It can be seen that the reduction and removal of frictional forces had an extremely large effect on crack growth rate, particularly at short crack lengths.

The use of pins with flats removes also the radial forces over a large area, but those close to the crack origin would be expected to retard the crack growth rate. Thus, the removal of frictional forces appears to be much more important than the removal of radial forces. This case is probably the closest practical one to the assumption made by Newman of a single load passing through the centre of the hole. The growth rate curves do in fact look similar, although they are displaced from one another. In addition they are both very different from the curve for the dry clearance fit pin, particularly at the shorter crack lengths, where the removal of frictional forces reduced the crack growth rate by approximately an order of magnitude. Therefore, in order to predict accurately the rate of crack growth in a lug these frictional forces must be included in the model used for the analysis. In order to do this, the magnitude and distribution of the radial and frictional forces around the hole must be known. The derivation of approximate distributions is described in the next section.

3 MECHANISM OF LOAD TRANSFER BETWEEN PIN AND LUG

Work which has been carried out analysing the stress distribution around the hole in a lug, ignoring frictional forces, has been reviewed¹. It was shown that the distribution of radial pressure is very dependent upon lug geometry, and no single expression can be used for all lugs. The results presented indicated that, for the lug geometry used in the crack propagation experiments described in section 2, a cosine distribution was a reasonable approximation for the radial pressure around the hole:

$$\text{Radial pressure } (\sigma_r) = \sigma_{r_{\max}} \cos \theta \quad [-90^\circ \leq \theta \leq 90^\circ]$$

where $\sigma_{r_{\max}}$ = maximum value of $\sigma_r = -\frac{4 \text{ pin force}}{\pi d t}$

and θ is measured from the top of the hole, as shown on Fig 12.

The radial stress acting on the hole surface is always negative.

However, the radial pressure cannot be considered in isolation for conditions where frictional forces are present, as these forces will produce a resultant force in the direction of pin load, as described in the first part of the Appendix. Therefore, the

magnitude of the radial pressure at all points around the hole will depend upon the total magnitude of the frictional forces. In their basic studies of fretting fatigue using plain specimens, Edwards and Cook² showed that alternating frictional forces increased, or built up, during constant amplitude loading. If these forces build up between the pin and hole surface in a lug then the radial pressure would be expected to change during load cycling as a result. The author has carried out an experiment which studied the magnitude of radial pressure at one point around the hole during load cycling, to provide further evidence of the existence of frictional forces. In addition, data was obtained which allowed an estimate to be made of the magnitude of the frictional forces.

As the work has been described in detail previously¹, it will only be briefly outlined here. As it is very difficult to measure radial pressure directly, it was decided to make strain gauge measurements on the faces of the lug near the hole. Strain gauges were bonded to a lug at the top of the hole ($\theta = 0^\circ$) on both faces approximately 1 mm from the hole edge, as shown in Fig 13. The lug was of the same design as those used in the crack propagation measurements described in section 2, and was made of 7075 T7351 material. The radial pressure has been shown to be near its maximum value at the point of measurement for this lug geometry¹. The photoelastic tests which were used further showed that the hoop stress was negative at the top of the hole and less than a quarter of the value of the radial pressure at this point. Therefore it was felt that unidirectional strain gauge measurements would give a good indication of radial pressure in this area. The lug was subjected to a load sequence which was designed to investigate the effect on radial pressure of cycling at the stress amplitude used in the crack propagation tests, ie a mean stress of 95 MN/m² with an alternating stress of 23 MN/m².

Some selected results from the experiment are presented in Fig 14, on which is plotted the strain gauge output against the applied load. It should be noted that the strain (X) axis for each cycle is displaced to improve clarity. Thus, each cycle has its own strain axis. The lug was first cycled between zero load and the maximum load in the crack propagation tests. The first strain vs load curve is shown as cycle A on Fig 14. Very similar cycles were produced by five further cycles of this amplitude, the only difference being a steepening of the initial gradient. Load cycling was then carried out at the amplitude of the crack propagation tests (95 ± 23 MN/m). The first strain vs load curve obtained is shown as cycle B of Fig 14. Cycle C of the same figure was produced following 2500 further cycles of the same amplitude. Comparing cycles B and C, the cycles between obviously had a large effect on the local strain history. The hysteresis loop closed up, and the strain range decreased by about one third. The slope of the graph changed markedly. It can be seen that the slope over most of the loading range of cycle A was approximately one half that of cycle C, the actual change in slope being 55%. Loading continued for a further 12500 cycles at the same amplitude, having a negligible effect on the strain history.

Referring to the earlier discussion, a likely explanation for the reduction in radial pressure range due to cycling is that alternating frictional forces do build up between the pin and hole surface, in a similar manner to the forces observed by Edwards and Cook on plain specimens with fretting pads². The form of the hysteresis loops on

Fig 14, showing the strain gauge output against pin load, suggest that the frictional forces in the lug were similar in nature to those observed in the basic fretting fatigue work on plain specimens in that they were in opposite directions at the maximum and minimum points in the load cycle. As described in the Appendix, at the maximum stress in the load cycle the resultant of the radial and frictional forces act in the same direction and thus the radial pressure around the hole is reduced by the presence of the frictional forces. At the minimum stress, the frictional forces are reversed, thus opposing the reduction in radial pressure due to the decreasing net stress. Thus it can be seen that alternating frictional forces lead to an overall reduction in the cyclic range of radial pressure by causing a reduction in the radial pressure around the hole at the maximum stress, and an increase in radial pressure at the minimum stress in the load cycle.

It was decided to ascertain theoretically whether a build up of frictional forces could explain the large observed changes in radial pressure. In order to do this, some approximation had to be made of the likely distribution of frictional and radial forces. First, it was assumed that the radial pressure followed a cosine distribution ($\sigma_r = \sigma_{r_{max}} \cos \theta$), as explained earlier. Thus the pressure at the maximum and minimum stress in the load cycle could be calculated in the absence of friction.

The next stage was to make an assumption concerning the likely distribution and magnitude of frictional forces. The work of Edwards and Cook² referred to earlier, in which they observed the variation in frictional forces throughout the load cycle, showed that the peak alternating coefficient of friction ($\mu = (\text{frictional force/radial force})$) rises with increasing relative slip to a maximum value of around unity. Therefore it was assumed that the maximum value of μ occurred near the origin of the crack where relative slip between the pin and hole surface is at its greatest. At the top of the hole, nearest the end of the lug, μ must be zero, as on either side of this point the frictional forces will be in opposite directions. Perhaps the simplest function to satisfy the above requirements is of the form $\mu = \mu_{max} \sin \theta$. Presented in the second part of the Appendix is the calculation process by which several values of μ_{max} were tried in order to assess the theoretical effect of fully reversed frictional forces on the range of radial pressure. It was found that high values of μ_{max} , ie approaching unity, led to the prediction that the radial pressure around the hole was greater at the minimum stress in the load cycle than that at the maximum stress. This prediction demonstrates the potentially large effect of frictional forces on radial pressure, but does not agree with the experimentally observed behaviour. In addition, this prediction does not appear to be a practical possibility because as the pin load reduces from the maximum to the minimum point, the relative slip between the pin and hole must lead to a reduction in radial pressure. It was found that a value of $\mu_{max} = 0.1$ was required to predict a reduction in radial pressure range of 33.4%, which is close to the experimentally observed figure of 33%. Thus, the presence of feasible distribution of alternating frictional forces can explain the reduction in radial pressure range (at all points around the hole) indicated by the measurements of radial strain described.

The work described in this section has provided further evidence of the presence of significant alternating frictional forces which build up during load cycling. Further, expressions for the distributions of radial pressure and frictional forces have been developed which fit the available information. These allow the effects of frictional forces to be included in a fracture mechanics analysis of a lug, the results of which are presented in the next section.

4 THEORETICAL PREDICTIONS OF CRACK PROPAGATION IN A LUG

4.1 Pins with flats

Newman has developed a solution to predict the growth rate of a corner crack from a hole in a finite width plate, which is subjected to a single load acting through the centre of the hole¹³. The result of using this solution to predict crack growth rate was plotted on Fig 11 and discussed in section 2.

The only aspect of lug geometry not modelled correctly in this solution is the distance from the hole to the end of the lug, measured in the direction of the (tensile) pin load. This distance is assumed to be infinite in the analysis. However, for the case of the lug under consideration, this distance is sufficiently large not to affect significantly (<5%) the stress concentration factor¹⁴, and is not considered to be important in the present analysis. Newman's solution was used to predict the value of $Y = (\Delta K / \sigma \sqrt{a})$ at various values of a/r for the geometry of lug used in the crack propagation tests, and the crack geometry observed in these tests. The predictions of Y are plotted against a/r on Fig 15, together with the experimentally derived values of Y for the nearest practical case of a lug loaded by a pin with flats, taken from section 2. As discussed in that section, the pin with flats used in the tests removed radial and frictional forces from around the crack origin and concentrated the load over a 12.7mm wide strip at the top of the 25.4mm diameter hole. It is therefore not quite the same as the single load acting through the centre of the hole assumed by Newman, but it is probably impossible to get nearer this model practically. It can be seen that there is reasonable agreement, Newman's solution resulting in values of Y about 14% greater than the experimental data over most of the range of a/r . Although it is possible that the experimental and theoretical curves should be further apart, owing to inaccuracies in the basic ΔK data discussed in section 2, the shape of the two curves is very similar. Therefore, it was decided that Newman's solution was a suitable starting point.

4.2 Clearance fit pin with lubricant

K can be calculated for the case of a crack at a hole, loaded by an arbitrary distribution of radial and frictional forces, in an infinite plate using a Green's function obtained by Muskhelishvili¹⁵. Although any distribution of radial and frictional forces can be modelled using this solution, it is not entirely appropriate for predicting crack growth in a lug since the finite dimensions of the lug, particularly width, are not modelled. However, it can be used to predict the effect of a change in the distribution of radial and frictional forces, which can be used to modify Newman's solution, which does model the finite width of the lug.

For example, Rooke's solution was used to calculate K_p and K_{\cos} for the case of a crack at a hole in an infinite plate:

where $K_p = K$ due to a point load (actually a uniform pressure over a very small arc at the top of the hole),

and $K_{\cos} = K$ due to a cosine distribution of radial pressure.

The value of Y predicted by Newman's solution at each chosen value of a/r was then multiplied by the ratio K_{\cos}/K_p , for the same value of a/r , to obtain an estimate of Y for a cosine distribution of radial pressure in the lug used in the crack propagation measurement experiments. Thus

$$\left(Y \text{ for a cosine distribution of radial pressure} \right) = (Y \text{ for a point load}) \times \frac{K_{\cos}}{K_p}.$$

Values of Y vs a/r , for a cosine radial pressure distribution, are plotted on Fig 16, along with values of Y for a point load, calculated using Newman's solution, taken from Fig 15. Also plotted on Fig 16 are the values of Y for the cases of a pin with flats and a lubricated pin, derived from the crack propagation experiments described in section 2. It was stated in section 2 that a review of available information¹ indicated that a cosine radial pressure distribution is a reasonable approximation for the lug geometry under consideration. If the lubricant removed all frictional forces, then the experimentally derived values of Y for a lug loaded by a lubricated pin might be expected to be close to the predictions for the case of a cosine radial pressure distribution with no friction. In practice, the lubricant will probably only reduce rather than remove frictional forces, and the experimental values of Y will therefore be higher. Nevertheless the two predictions of Y plotted on Fig 16, ie for a point load and a cosine radial pressure distribution, may be considered to correspond to the two experimentally derived results, for a pin with flats and a lubricated pin. Examination of Fig 16 shows that the effect of adjusting Newman's solution to allow for a cosine radial pressure distribution, as described earlier, is to increase Y for $a/r < 0.15$ and decrease Y for larger a/r . This behaviour is also seen when comparing the experimental cases, the crossover of curves taking place at almost exactly the same relative crack length. At short crack lengths, $0.1 < a/r < 0.2$, the difference in the experimental curves is much greater than between the predictions. This is probably due to the lubricant only reducing rather than removing frictional forces, as mentioned above.

4.3 Clearance fit pin without lubricant

The analysis is now extended to include the action of frictional forces. In section 3 the following distributions of radial and frictional forces around the hole were developed for the lug geometry and loading level under consideration:

$$\text{Radial pressure } (p_r) = p_{r_{\max}} \cos \theta \quad (-90^\circ \leq \theta \leq 90^\circ) \quad (2)$$

$$\text{Alternating coefficient of friction } (\mu) = 0.1 \sin \theta \quad (-90^\circ \leq \theta \leq 90^\circ) \quad (3)$$

It was assumed that the frictional forces acted in opposite directions at the maximum and minimum points in the load cycle. This assumption brings with it the necessity to calculate K at both the maximum and minimum points in the load cycle in order to calculate ΔK . In the previous calculations of Y (normalised ΔK), when no friction was assumed, this procedure was unnecessary because K at any point in the load cycle was directly proportional to the applied stress. Thus, for the previous case with no friction:

$$\frac{K_{\max}}{\sigma_{\max} \sqrt{\pi a}} = \frac{K_{\min}}{\sigma_{\min} \sqrt{\pi a}} = \frac{\Delta K}{\sigma_g \sqrt{\pi a}} \quad (4)$$

where $\sigma_g = (\sigma_{\max} - \sigma_{\min})/2$

and $\Delta K = (K_{\max} - K_{\min})/2$.

NB Throughout this Report, the symbols σ_g and ΔK are used to define the alternating semi-range of gross section stress and stress intensity factor respectively.

However, with alternating frictional forces, the frictional component has to be added to the radial pressure component of K separately at the maximum and minimum points of the load cycle in order to determine ΔK . Thus, for the present case with alternating frictional forces:

$$Y = \frac{K_{\max} - K_{\min}}{2\sigma_g \sqrt{\pi a}} = \frac{\Delta K}{\sigma_g \sqrt{\pi a}} \quad (5)$$

This point will become more clear later in this section when the calculation process is described in detail, and the results are discussed.

Rooke's solution was used to calculate the maximum and minimum values of K for the same stress ratio (R) used in the crack propagation tests, assuming a cosine radial pressure distribution, with and without friction, in a hole in an infinite plate. In order to aid the following description, the stages in the calculation process are shown on Fig 17, parts (a) and (b) being for the maximum and minimum points in the load cycle respectively. Plotted on this graph are values of K/K_b vs a/r ,

$$\text{where } K_b = \sqrt{\pi a} \left(\frac{\text{pin load at maximum stress in load cycle}}{dt} \right) \quad (6)$$

The continuous lines on both graphs show the values of K/K_b at the maximum and minimum points of the load cycle for a cosine radial pressure distribution with no friction. At any value of a/r :

$$K_{\min} = R \times K_{\max} \quad (7)$$

In order to avoid confusion it should be emphasized that Fig 17 cannot be compared directly with Figs 15 and 16 as these two Figures present predictions of Y for a finite width lug whereas Fig 17 presents predictions for an infinite plate.

The effect of frictional forces at maximum load is to reduce radial pressure at all points around the hole and therefore K due to radial pressure alone will be reduced, as shown by the dotted square symbols on Fig 17a. At the minimum load, the frictional forces act in the opposite direction, leading to an increase in radial pressure and consequently an increase in K due to radial pressure, shown on Fig 17b, again with dotted square symbols.

At maximum load, the frictional forces act to produce a positive contribution to K , shown by the cross symbols on Fig 17a. As the frictional forces act in the opposite direction at the minimum load, they will contribute a negative component to K , shown by the crossed symbols on Fig 17b.

The net result of the contributions due to radial pressure and frictional forces is shown by the dotted circle symbols on Fig 17a&b. It can be seen that the net effect of frictional forces is to increase K for all values of a/r at the maximum load and to reduce K at the minimum load. The resulting increase in ΔK due to the inclusion of the action of frictional forces is shown on Fig 18. The values of K/K_b for the maximum and minimum points of the load cycle for the cases with and without friction, are plotted against a/r on this Figure. The K/K_b axis is magnified compared with the previous Figure in order to improve clarity. The results plotted on Fig 18 were used to calculate the percentage increase in both ΔK and K_{\max} due to the inclusion of the effect of frictional forces:

$$\% \text{ increase in } \Delta K = \left[\frac{\Delta K(\text{with friction})}{\Delta K(\text{without friction})} - 1 \right] \times 100 \quad (3)$$

$$\% \text{ increase in } K_{\max} = \left[\frac{K_{\max}(\text{with friction})}{K_{\max}(\text{without friction})} - 1 \right] \times 100 \quad (9)$$

The calculated percentage increases in ΔK and K_{\max} are plotted against a/r in Fig 19. It can be seen that ΔK is increased by between 47% at $a/r = 0.01$ and 16% at $a/r = 1.00$ for the case of a loaded hole in an infinite plate. In contrast, K_{\max} is increased by between only 10% and 4% over the same range of a/r .

In order to obtain a prediction for the finite width lug used in the experiments, it was assumed that frictional forces had the same effect on ΔK in both a finite and infinite width plate. The value of Y for a cosine distribution of radial pressure with no frictional forces around a hole in a finite width lug (Fig 16) was multiplied by the ratio of ΔK with and without friction, calculated using Rooke's solution:

$$\underbrace{Y(\text{for radial pressure and frictional forces})}_{\text{prediction for a lug with a normal pin}} = \underbrace{Y(\text{for a cosine radial pressure distribution})}_{\text{prediction ignoring friction}} \times \underbrace{\frac{\Delta K(\text{with friction})}{\Delta K(\text{without friction})}}_{\text{obtained using Rooke's solution}} \quad (10)$$

The resulting values of Y , including the action of frictional forces, are plotted against a/r on Fig 20, together with the two previously described predictions of Y which ignore frictional forces.

It should be emphasized that the prediction including the action of frictional forces is for the particular lug used in the crack growth experiments under the prescribed loading conditions. A different answer would be expected for other conditions. For example, relative slip in a larger lug would be greater, leading to a probable increase in frictional forces, and increased alternating load would lead to increased slip and hence frictional forces. Increased frictional forces would lead to a greater reduction in radial pressure range. Thus, the contribution to ΔK due to radial pressure would be reduced and that due to frictional forces would be increased, and the total calculated ΔK would therefore be different from the case considered in this section.

Examination of Fig 20 shows that the prediction which includes the action of frictional forces gives the closest agreement with the experimental result for a dry clearance fit pin in the important region of short crack lengths. In order to present more clearly the difference in accuracy between the predictions with and without the inclusion of the effect of frictional forces, the results presented in Fig 20 were used to calculate the errors in the prediction for ΔK when compared with the experimental result. This was achieved by plotting the value of

$$\left(\frac{Y_{\text{exp}} - Y_{\text{cal}}}{Y_{\text{exp}}} \times 100 \right) \% \text{ vs } \frac{a}{r} \text{ on Fig 21}$$

where Y_{exp} = Y derived from L65 experimental data for a clearance fit pin with no lubricant

Y_{cal} = calculated value of Y .

The a/r scale (X axis) is magnified compared with Fig 20 to concentrate on the important region of short crack lengths. It can be seen that there is a large improvement in accuracy for $a/r < 0.1$. However, for longer crack lengths, with $a/r > 0.2$, the inclusion of the effect of frictional forces leads to an overestimation of Y of approximately 30%.

It should be noted that in the predictions it was assumed that the radial and frictional forces remain constant throughout the entire cracked life, whereas the finite element results of Hau¹⁶ and Callinan¹⁷ indicate that there are significant changes in radial pressure distribution as the crack grows longer. The consequent possibilities of inaccuracies in the predictions made will however be reduced to some extent by the fact that as the crack tip becomes more remote from the points of application of load, the type of distribution assumed becomes less important. No attempt was made to allow for this effect, as it is the growth of short cracks which is of most interest owing to the fact that this phase normally occupies the majority of fatigue life. Furthermore, the anomaly between theory and experimental evidence discovered previously was at short crack lengths, so the analysis concentrated on this area.

4.4 Sensitivity of prediction to assumed distribution of frictional forces

In order to include the effect of frictional forces in a fracture mechanics analysis, a relatively simple approximation, concerning the magnitude and distribution of these forces, was made, which fitted the limited available information. A more accurate description of the actual radial and tangential forces around the hole surface should reduce the error in predicting crack growth rate. It was decided to make an assessment of the sensitivity of the prediction to the nature of the assumption regarding the frictional force distribution. It is possible that frictional forces build up relatively more, close to the origin of the crack, than at other points of contact owing to large amounts of relative slip taking place in that area. This is evidenced by the fretting marks on the surface of the hole at the minimum section in the area of crack initiation. In the case of the lug under consideration these marks can be up to 3mm wide.

Making the assumption that μ_{\max} increases locally from 0.3 to 0.6 over a 14° arc (3.1mm long), the previously described method was used to determine the resulting change in ΔK . It was found that ΔK (compared with the case for $\mu = 0$) was increased by between 30% at $a/r = 0.01$ and 11.5% at $a/r = 0.30$, as shown on Fig 22. If the arc over which the frictional forces are increased is reduced to only 4° (0.9mm long), it is found that a much smaller range of crack length is affected to such a large extent. For example, if the frictional forces are increased by a factor of 5 over a 4° arc, producing a 30% increase in ΔK at $a/r = 0.01$, the increase in ΔK is less than 11% at $a/r = 0.08$. A value of $\mu = 1.5$ does not appear to be practical but was assumed to aid comparison as it produces a similar effect on ΔK at $a/r = 0.01$ to the assumption that μ is doubled over a 14° arc. However, frictional forces of the same magnitude could exist with more feasible values of μ , i.e. less than unity, if the radial pressure over this small region was higher than given by the assumption made of a cosine distribution. This could result from the hole elongating under loading and 'wrapping around' the pin at the lug minimum section. It can be seen from Fig 22 that the nature of the frictional forces close to the crack origin has a large effect on ΔK at short crack lengths; the closer the forces are to the origin of the crack, the shorter the crack length affected.

This conclusion suggests that the prediction of the experimentally derived result for a dry clearance fit pin could be made more accurate, than that plotted on Fig 20, if a different assumption for the distribution of μ was made. If μ built up relatively more close to the origin of the crack than given by the assumption made of $\mu = 0.3 \sin \theta$, and relatively less at points away from the crack origin near the top of the hole, then the predicted increase in ΔK due to frictional forces would be greater at low values of a/r and smaller at high values of a/r . The predicted values of Y would then be much closer to the experimentally desired result over the full range of a/r than those shown on Fig 20. However, there is no further information available at this time on which to base a suitable distribution of μ around the hole. Further work should be carried out to help define a more accurate distribution of radial and tangential forces under fretting conditions.

5 CONCLUDING REMARKS

In a previous Report by the author experimental ΔK distributions were presented, derived from crack propagation rate measurements of corner cracks for the case of a lug loaded by a clearance fit pin. It was found that the crack grew much faster (by approximately an order of magnitude) at short crack lengths than predicted by available fracture mechanics solutions. Examination of the findings of basic studies of fretting fatigue strongly suggested that this difference between predicted and observed growth rate was due to the action of frictional forces between the pin and hole surface, which are normally ignored in theoretical analyses.

In order to substantiate this hypothesis, crack propagation rate measurements have been carried out on lugs in which frictional forces were reduced by lubrication and eliminated from around the origin of the crack by the use of pins with flats. It was found that in addition to extending the life to the initiation of a small crack (around 0.5 mm), the reduction and removal of frictional forces led to a very large fall in propagation rate over the shorter crack lengths (up to around 6 mm or $a/r = 0.5$).

Previously reported measurements of radial strain on the face of the lug at the top of the hole indicated that the range of radial pin pressure decreased during load cycling owing to a build up of frictional forces which share the pin load with the radial pressure. From an examination of the results of these measurements it was concluded that these frictional forces were alternating in nature, i.e. they acted in opposite directions at the maximum and minimum points in the load cycle. Thus, at maximum load they act to cause a reduction in radial pressure around the hole, and at minimum load they are reversed, thus opposing the reduction in radial pressure due to the decreasing pin load. The total range of radial pressure is thereby reduced. The radial strain measurements, together with information on radial pin pressure distributions derived from the literature, allowed an estimate to be made of the actual distribution of radial and tangential forces in a lug. It was found that including the effects of alternating frictional forces, rather than considering radial pressure only, in a fracture mechanics analysis of a lug led to a significant increase in ΔK , and hence crack growth rate, at short crack lengths. The increase in ΔK was found to be much greater than the increase in the maximum value of K . The sensitivity of the prediction to the form of the assumed frictional force distribution was assessed and it was found that the magnitude of the forces very close to the crack origin was particularly important, governing the growth of short cracks.

The experimentally observed results of using lubricated pins and pins with flats could be predicted with reasonable accuracy, and good agreement for the case of a normal dry pin was achieved at short crack lengths, up to approximately 1 mm. However, at longer crack lengths the predictions of ΔK were between 20-30% higher than the experimentally derived results. This is probably due to a lack of knowledge of the actual distributions of radial and tangential forces, at the start of crack growth, and the way in which these forces change with increasing crack length. It was demonstrated that closer agreement between theory and experiment could be achieved if it was assumed that

the frictional forces built up relatively more, close to the crack origin, and relatively less, at points distant from the origin, than defined by the assumption made of $\mu = 0.3 \sin \theta$.

Appendix

LOAD TRANSFER BY RADIAL PRESSURE AND FRICTIONAL FORCES

A.1 Contribution of frictional forces to pin load

A schematic diagram is presented on Fig 23a of the radial and frictional forces acting on the hole surface in a lug with the pin load increasing and approaching its maximum value in the cycle. As shown, the frictional forces act in opposite directions on either side of the top of the hole and produce a resultant force in the direction of the movement of the pin relative to the lug. Thus, the resultant forces due to both the radial pressure and frictional forces act in the direction of the pin load, i.e. upwards on Fig 23a, through the centre line of the hole. Therefore, the introduction of frictional forces leads to a reduction in the radial pressure around the hole for this load case. By symmetry, the resultant horizontal force (at right angles to the direction of the pin load) due to the radial and frictional forces must be zero.

The directions of the radial and frictional forces acting on the hole surface with the pin load reducing and approaching its minimum value are presented on Fig 23b. It can be seen that the frictional forces have reversed in direction, compared with those on Fig 23a, and act to produce a resultant force downwards, in the direction of the movement of the pin relative to the hole. As the direction of the resultant of the frictional forces acts in the opposite direction to that of the radial forces, the introduction of frictional forces leads to an increase in radial pressure around the hole at the minimum stress in the load cycle. The load cycle considered is shown in the insert to Fig 23 and is wholly tensile, as in the crack propagation experiments.

The principles outlined in the description above are demonstrated in section 2 of this Appendix, in which the effects of two assumed distributions of frictional forces on the radial pressure around the hole are calculated.

A.2 Calculation of the effect of friction on radial pressure

Referring to Fig 24 and resolving the vertical load (dF) acting on the small element of the hole surface subtended by the angle $d\theta$.

For unit thickness:

$$dF = (\sigma_r \cos \theta + \tau \sin \theta) r d\theta \quad (A-1)$$

where τ is the shear stress due to the frictional force coefficient of friction (μ) = τ/σ_r .

Using the assumptions made in section 3

$$\sigma_r = \sigma_{r_{max}} \cos \theta$$

$$\mu = \mu_{max} \sin \theta$$

Substituting for τ , σ_r and μ given:

$$dF = \sigma_{r_{max}} r [\cos^2 \theta + \mu_{max} \sin^2 \theta \cos \theta] d\theta \quad (A-2)$$

$$\text{Total pin force (F)} = \sigma_{r_{\max}} r \int_{-\pi/2}^{\pi/2} \cos^2 \theta + \mu_{\max} \sin^2 \theta \cos \theta d\theta \quad (\text{A-3})$$

$$= \sigma_{r_{\max}} r \int_{-\pi/2}^{\pi/2} \left(\frac{1 + \cos 2\theta}{2} \right) + \mu_{\max} \sin^2 \theta \cos \theta d\theta \quad (\text{A-4})$$

$$= \sigma_{r_{\max}} r \left[\frac{\theta}{2} + \frac{\sin 2\theta}{4} + \frac{\mu_{\max} \sin^3 \theta}{3} \right]_{-\pi/2}^{\pi/2} \quad (\text{A-5})$$

$$\text{therefore} \quad F = \sigma_{r_{\max}} r \left[\frac{\pi}{2} + \frac{2\mu_{\max}}{3} \right] \quad (\text{A-6})$$

Example 1

Let $\mu_{\max} = 1$ and substituting into equation (A-6). At the maximum stress in the load cycle the frictional forces act in the direction shown on Fig 23a.

$$\text{Therefore} \quad \sigma'_{r_{\max}} \text{ (with friction)} = \frac{F_{\max} \text{ (maximum load)}}{r[\pi/2 + 2/3]} \quad (\text{A-7})$$

$$\text{and} \quad \sigma^2_{r_{\max}} \text{ (no friction)} = \frac{F_{\max}}{r[\pi/2]} \quad (\text{A-8})$$

$$\text{therefore} \quad \frac{\sigma'_{r_{\max}} \text{ (with friction)}}{\sigma^2_{r_{\max}} \text{ (no friction)}} = \frac{\pi/2}{\pi/2 + 2/3} = 0.70 \quad (\text{A-9})$$

Thus, the presence of frictional forces, defined by $\mu = \sin \theta$, leads to a 30% reduction in the value of $\sigma_{r_{\max}}$ at the maximum stress in the load cycle.

At the minimum stress in the load cycle, the frictional forces act in the direction shown on Fig 23b, assuming fully reversed frictional forces.

$$\text{Therefore} \quad \sigma^3_{r_{\max}} \text{ (with friction)} = \frac{F_{\min} \text{ (minimum load in cycle)}}{r[\pi/2 - 2/3]} \quad (\text{A-10})$$

Note the change in sign of the $2\mu/3$ term in the denominator.

$$\sigma^4_{r_{\max}} \text{ (no friction)} = \frac{F_{\min}}{r(\pi/2)} \quad (\text{A-11})$$

therefore

$$\frac{\sigma_{r_{\max}}^3 \text{ (with friction)}}{\sigma_{r_{\max}}^3 \text{ (no friction)}} = \frac{\pi/2}{[\pi/2 - 2/3]} \quad (\text{A-12})$$

$$= 1.74$$

Thus, at the minimum stress in the load cycle, the presence of frictional forces leads to an increase of 74% in $\sigma_{r_{\max}}$.

For the load cycle used in the crack propagation tests and in the radial strain measurements described in section 3:

$$R = \frac{F_{\min}}{F_{\max}} = 0.62$$

Substituting into equation (A-10), at the minimum stress in the load cycle

$$\sigma_{r_{\max}}^3 \text{ (with friction)} = \frac{0.62 F_{\max}}{r[\pi/2 - 2/3]} = \frac{0.685 F_{\max}}{r}$$

At the maximum stress in the load cycle, equation (A-7) gives:

$$\sigma_{r_{\max}}' \text{ (with friction)} = \frac{0.447 F_{\max}}{r}$$

Thus, it can be seen that the assumption of the presence of alternating frictional forces, defined by $\mu = \sin \theta$, in conjunction with a radial pressure distribution defined by $\sigma_r = \sigma_{r_{\max}} \cos \theta$, leads to the prediction that the radial pressure around the hole is greater at the minimum stress than at the maximum stress in the load cycle. This is a much larger effect than observed experimentally, therefore a lower value of μ_{\max} is assumed in Example 2.

Example 2

Let

$$\mu_{\max} = 0.3$$

At the maximum stress in the load cycle, substitution for μ in equation (A-6) gives:

$$\sigma_{r_{\max}}' \text{ (with friction)} = \frac{F_{\max}}{r[\pi/2 + 0.2]} = \frac{0.565 F_{\max}}{r}$$

$$\sigma_{r_{\max}}^2 \text{ (no friction)} = \frac{F_{\max}}{r[\pi/2]} = \frac{0.636 F_{\max}}{r}$$

At the minimum stress in the load cycle, again for $R = 0.62$ and assuming fully reversed frictional forces:

$$\sigma_{r \max}^3 \text{ (with friction)} = \frac{0.62F_{\max}}{r[\pi/2 - 0.2]} = \frac{0.452F_{\max}}{r}$$

$$\sigma_{r \max}^4 \text{ (no friction)} = \frac{0.62F_{\max}}{r[\pi/2]} = \frac{0.395F_{\max}}{r}$$

therefore

$$\begin{aligned} \text{radial pressure range (no friction)} &= (0.636 - 0.395) \frac{F_{\max}}{r} \\ &= \frac{0.241F_{\max}}{r} \end{aligned}$$

$$\begin{aligned} \text{radial pressure range (with friction)} &= (0.565 - 0.452) \frac{F_{\max}}{r} \\ &= \frac{0.113F_{\max}}{r} \end{aligned}$$

Therefore

$$\begin{aligned} \text{percentage change in radial pressure range due to friction} &= \frac{0.241 - 0.113}{0.241} \times 100 \\ &= 53.4\% \end{aligned}$$

This is very close to the experimentally observed reduction in radial pressure range of 55%.

LIST OF SYMBOLS

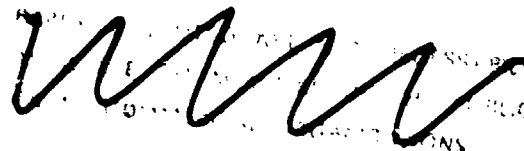
A	Head height of lug = distance from centre of hole to end of lug
K	stress intensity factor
K_b	K based on maximum pin bearing stress in cycle
K_{max}	maximum value of K in cycle
K_{min}	minimum value of K in cycle
K_c	fracture toughness
K_p, K_{cos}	K due to point and cosine distribution of load respectively
R	stress ratio = (minimum stress)/(maximum stress) in constant amplitude fatigue test
W	width of lug
Y	stress intensity coefficient or correction factor = $(\Delta K)/(\sigma_g \sqrt{\pi a})$
a	crack length
d	diameter of hole in lug
da/dN	crack propagation rate (length per cycle)
r	radius of pin
t	thickness of lug
ΔK	semi-range of alternating K = $(K_{max} - K_{min})/2$
θ°	angle subtended at hole centre, measured from head of lug
τ	shear stress
μ	coefficient of friction
σ_g	semi-range of alternating gross section stress = (alternating load)/(wt)
σ_r	radial pin pressure
$\sigma_{r_{max}}$	maximum value of σ_r

REFERENCES

- | <u>No.</u> | <u>Author</u> | <u>Title, etc</u> |
|------------|--|--|
| 1 | J.E. Moon | Crack growth in pin loaded lugs.
Paper presented at the 11th ICAF Symposium Noordwijkerhout,
The Netherlands, May 1981.
Also RAE Technical Report 82023 (1982) |
| 2 | P.R. Edwards
R. Cook | Fracture mechanics prediction of fretting fatigue under constant
and variable amplitude loading.
Presented at 11th Congress of ICAS, September 1978, Lisbon,
Portugal |
| 3 | G. Leadbeater
V.V. Kovalevskii
B. Noble
R.B. Waterhouse | Fractographic investigation of fretting-wear and fretting
fatigue in aluminium alloys.
Fatigue of Eng. Materials and Structures, Vol 3, pp 237-246 |
| 4 | R.M.G. Meek | Effect of pin bending on the stress distribution in thick plates
loaded through pins.
NEL Report No. 311, August 1967 |
| 5 | J. Schijve
F.A. Jacobs | The fatigue strength of aluminium alloy lugs.
NLL-TN M2024. ICAF Doc. 99 (1957) |
| 6 | P.R. Edwards
R. Cook | Effect of dewatering penetrant on frictional forces under
fretting conditions.
Unpublished RAE material |
| 7 | J.E. Moon | Improvement in the performance of pin-loaded lugs.
RAE Technical Report 80148 (1980) |
| 8 | P.R. Edwards | A computer program for the interpolation and extrapolation of
crack propagation data.
RAE Technical Report 76115 (1976) |
| 9 | S. Maddox | Research on the effect of mean stress and residual stress on the
rate of propagation of fatigue cracks.
Welding Institute Report 3356/9/74 (1974) |
| 10 | N.E. Frost
L.P. Fook
K. Denton | A fracture mechanics analysis of fatigue crack growth data for
various materials.
NEL A2/1/69 (1969) |
| 11 | S. Pearson | Initiation of fatigue cracks in commercial aluminium alloys and
subsequent propagation of very short cracks.
Eng. Fracture Mechanics, Vol 7, pp 235-247, 1975.
Also RAE Technical Report 72236 (1972) |
| 12 | J.E. Moon
P.R. Edwards | Fatigue behaviour of pin-loaded lugs of MS2L65 aluminium alloy.
RAE Technical Report 77167 (1977)
Also ARC R&M 1834 |

REFERENCES (concluded)

- | <u>No.</u> | <u>Author</u> | <u>Title, etc</u> |
|------------|--------------------------------------|---|
| 13 | J.C. Newman, Jr | Predicting failure of specimens with either surface cracks or corner cracks at holes.
NASA TN D-8244, June 1976 |
| 14 | Engineering
Sciences Data
Unit | Stress concentration factors. Axially loaded lugs with clearance fit pins.
Engineering Sciences Data Item No.81006 |
| 15 | D.P. Rooke
S.M. Hutchins | Stress intensity factors for cracks at loaded holes - effect of load distribution.
RAE Technical Report 82054 (1982) |
| 16 | T.M. Hsu | Analysis of cracks at attachment lugs.
Presented at the AIAA/ASME 21st Structures, Structural Dynamics and Materials Conference, 12-14 May 1980, in Seattle, Washington. |
| 17 | R.J. Callinan | Residual strength of a cracked lug.
Aeronautical Research Laboratories, Structures Note 442, 1977. Melbourne, Australia. |



Scale 1
 Nominal dimensions in mm
 Material - BS 2L 65 aluminium alloy

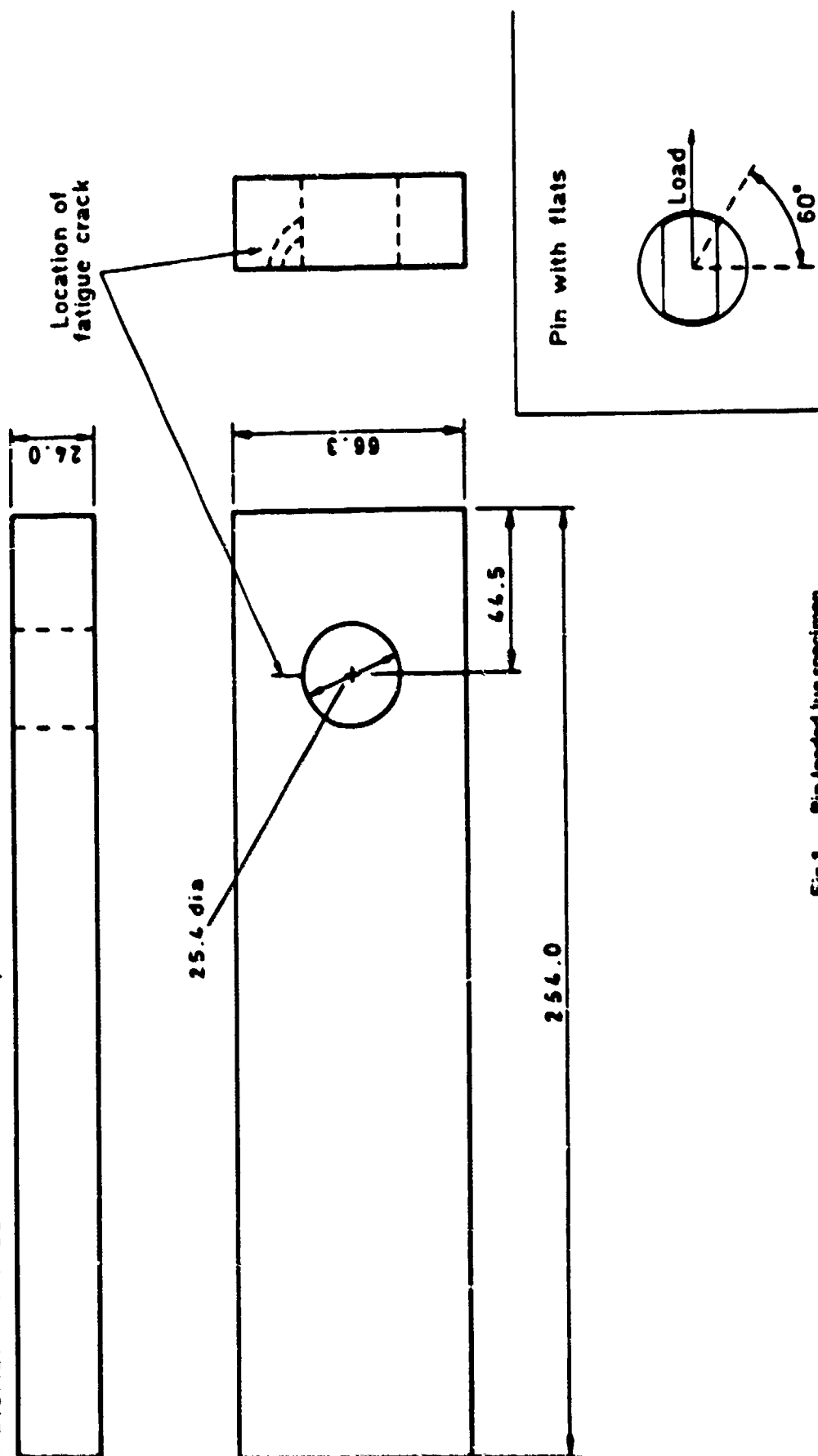


Fig 1 Pin-loaded lug specimen

Fig 2

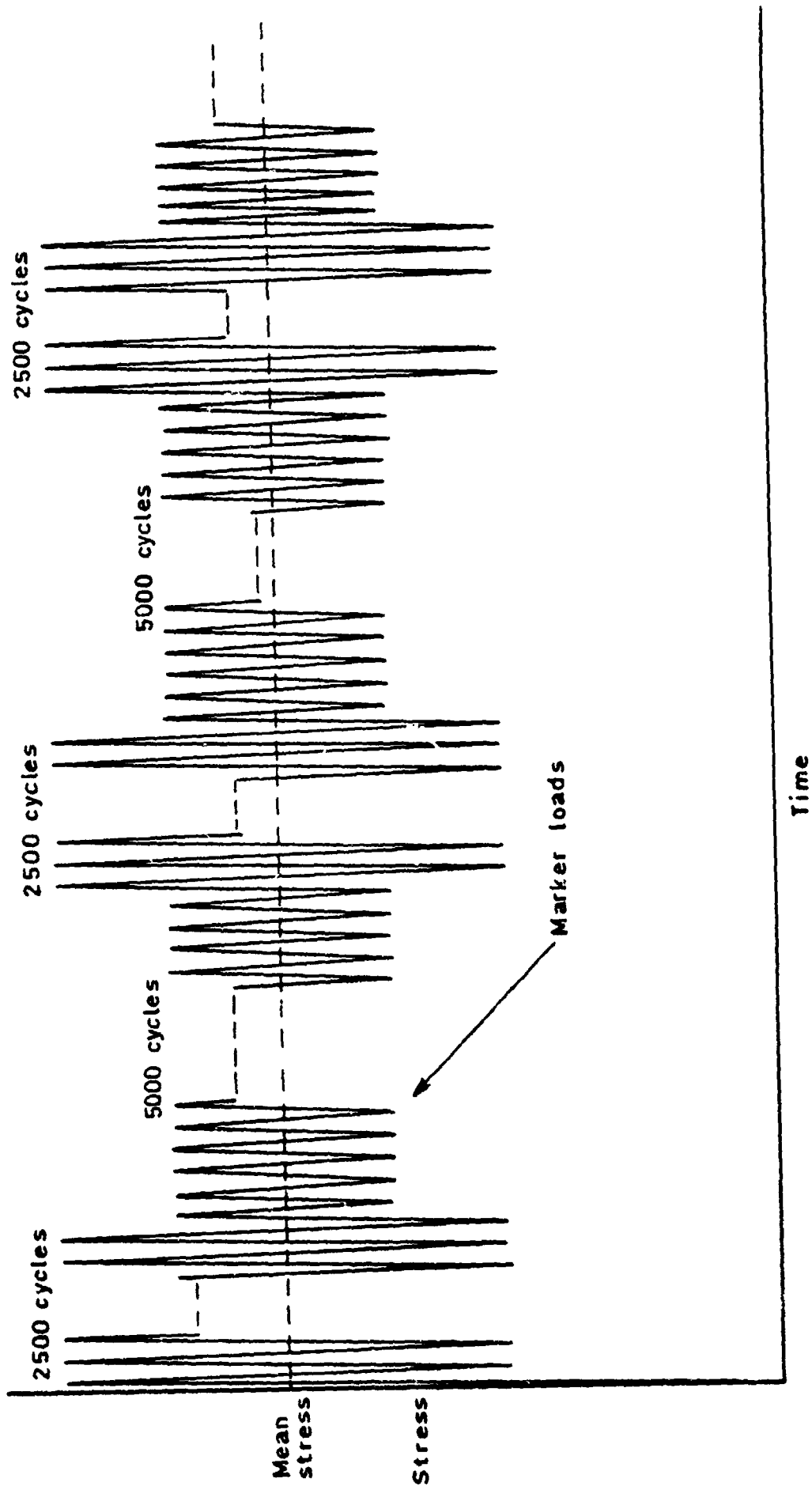


Fig 2 Schematic diagram of 2 level block programme used in crack propagation experiments

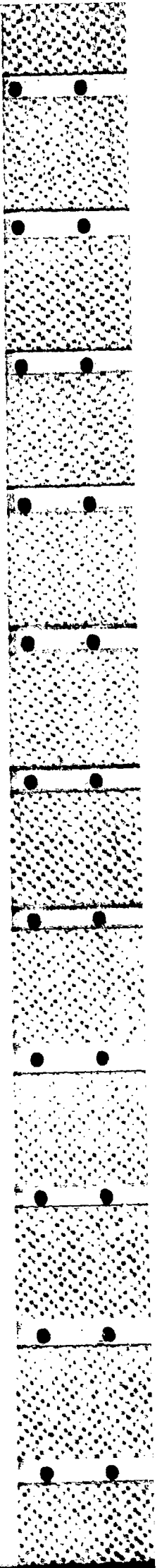




Fig 3 Photomicrograph of fracture surface showing marker lines

Fig 4

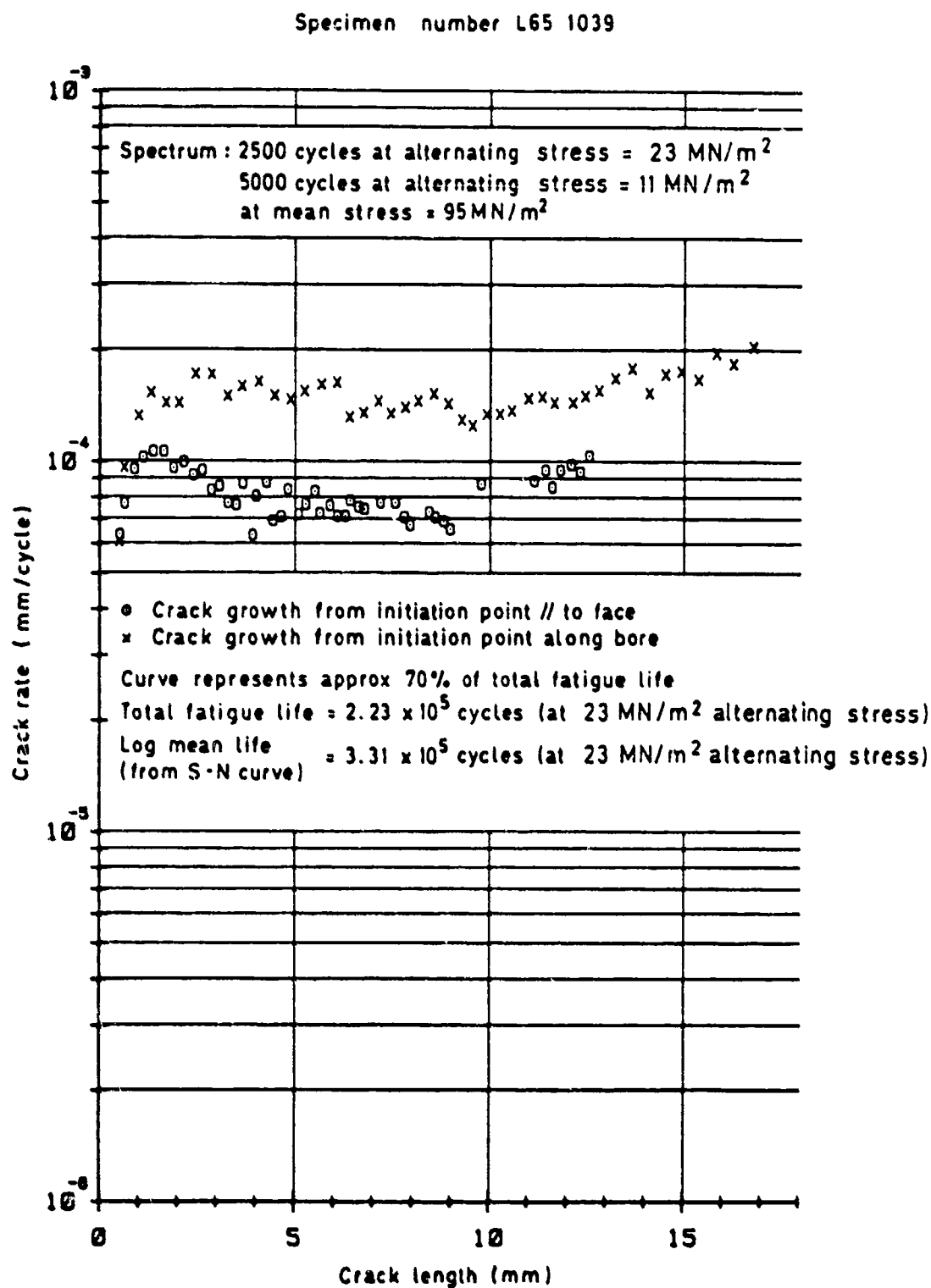


Fig 4 Crack propagation curve for a lug loaded by a clearance fit pin with no lubricant under constant amplitude loading

Fig 5

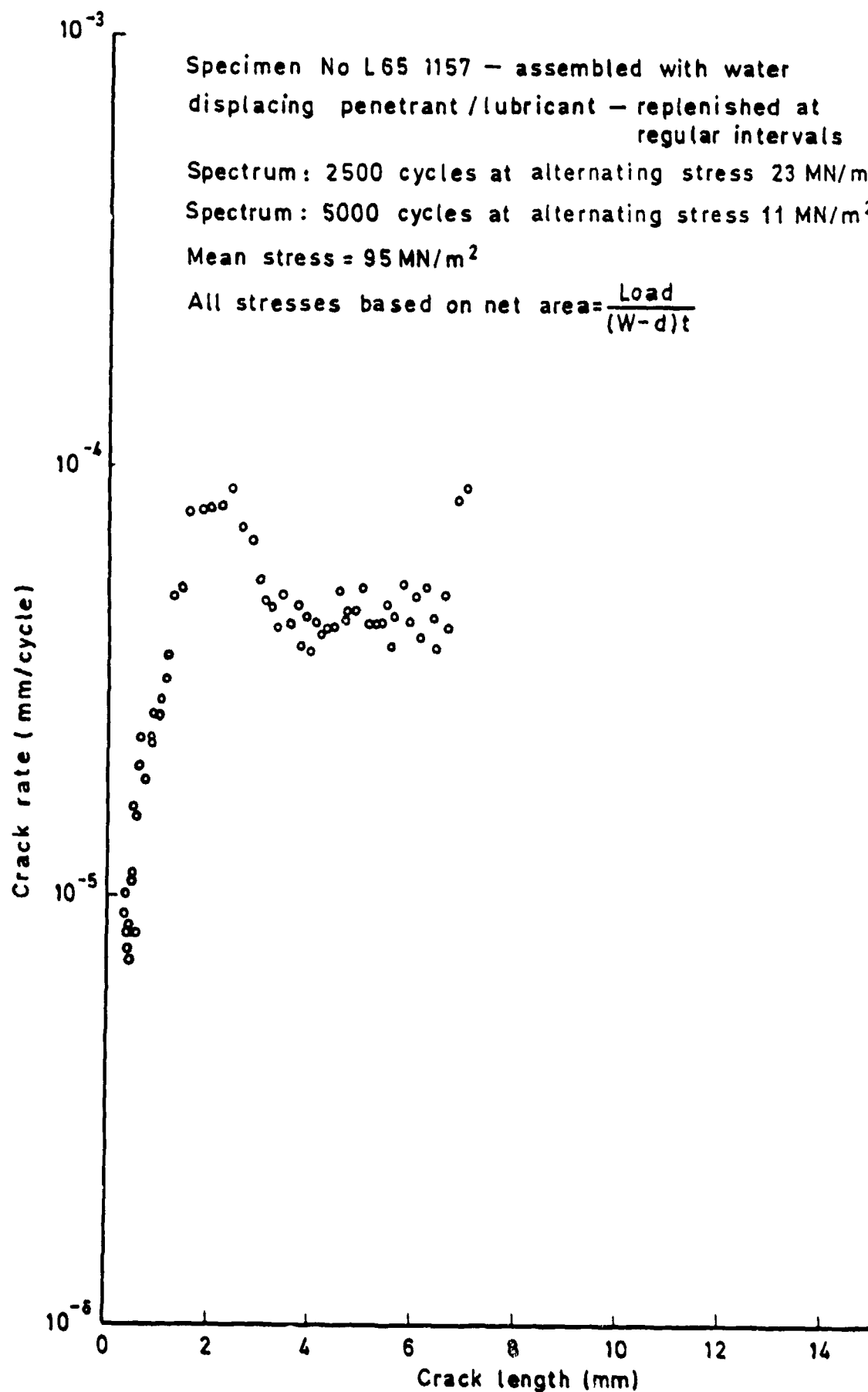


Fig 5 Crack propagation curve for lug with lubricated pin

Fig 6

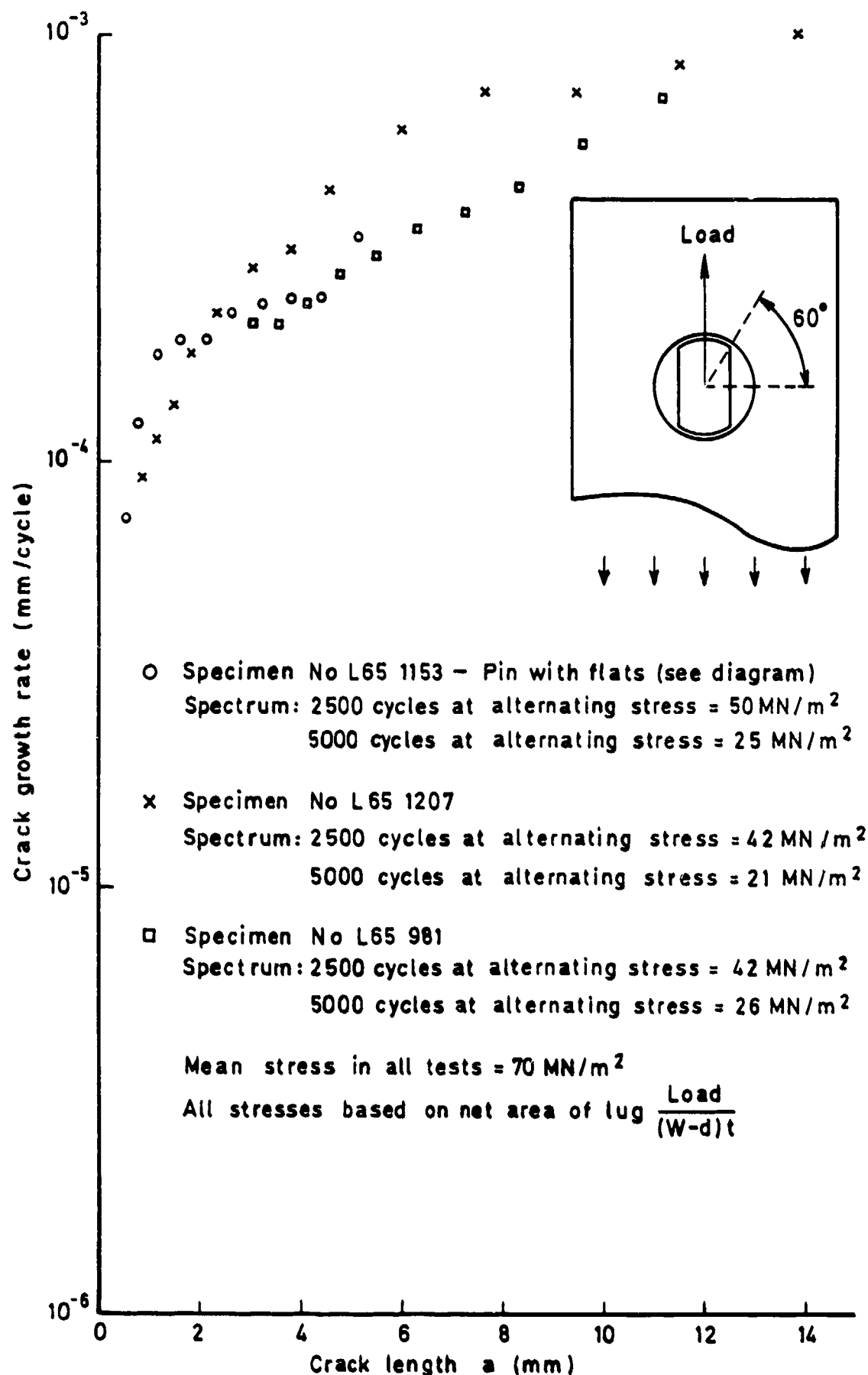


Fig 6 Crack propagation curve for a lug loaded by a pin with flats

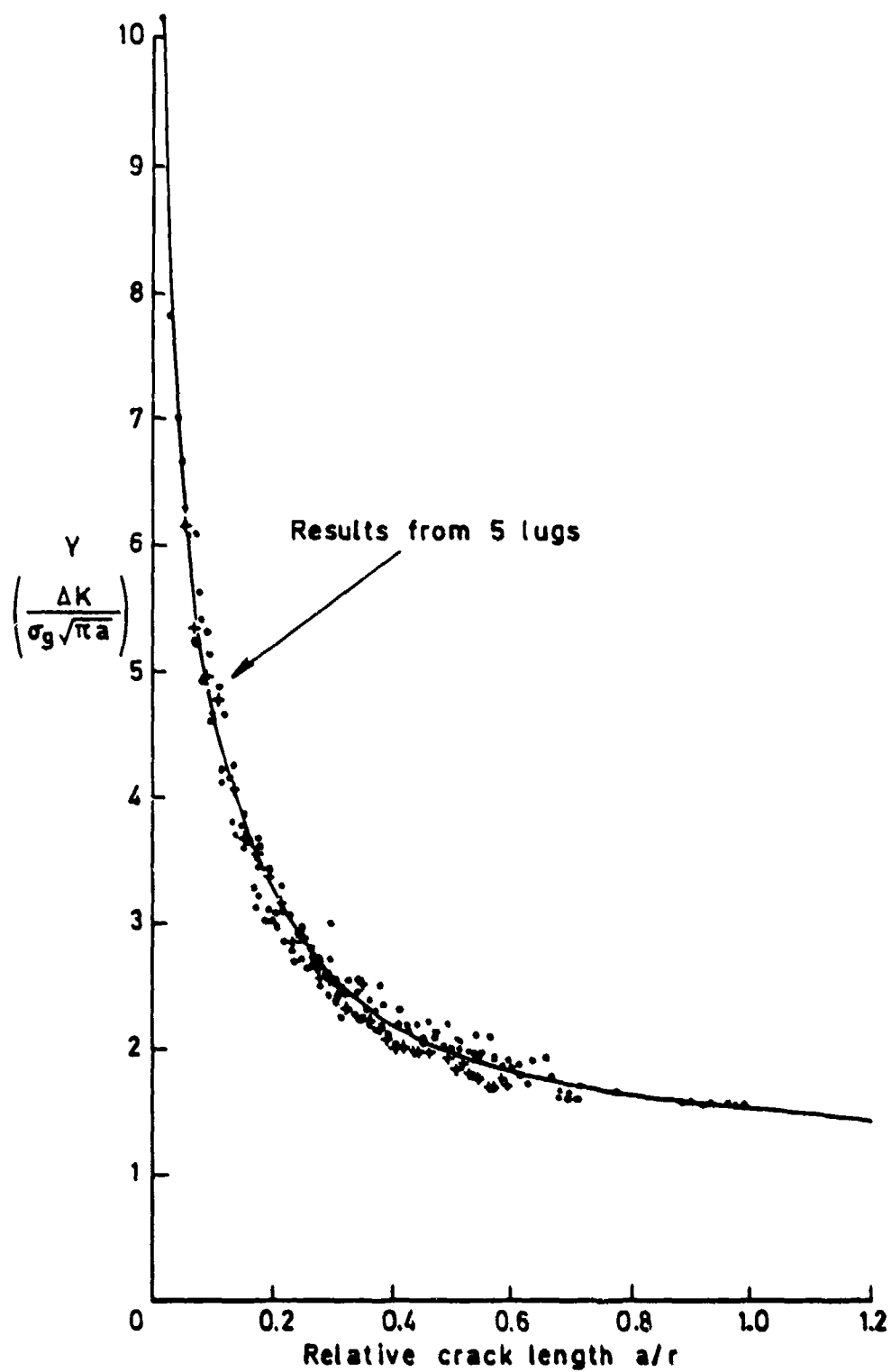


Fig 7 Stress intensity factor coefficient for a lug loaded by a clearance fit pin with no lubricant

Fig 8

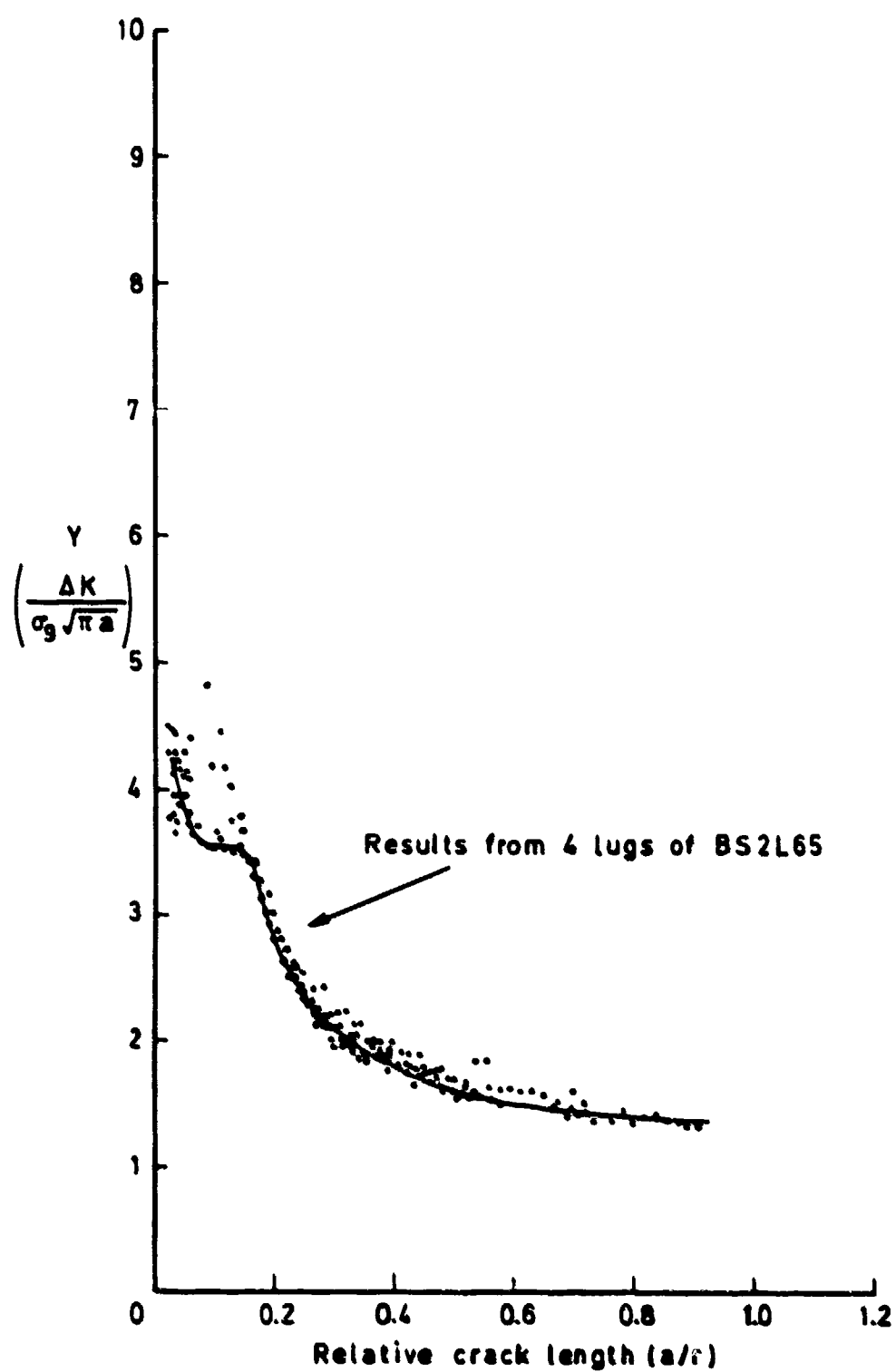


Fig 8 Stress intensity factor coefficient for a lug with a lubricated pin

Fig 9

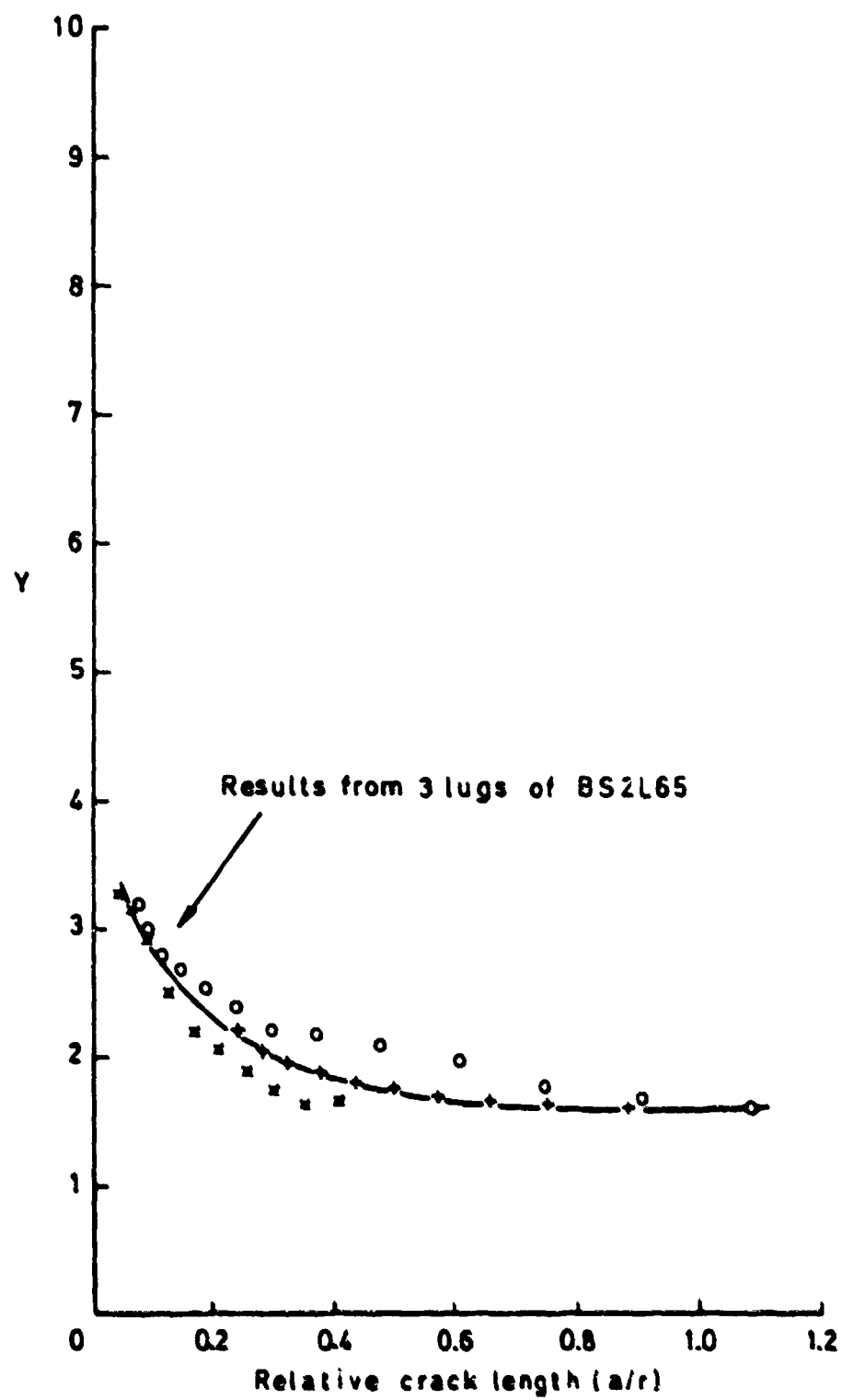


Fig 9 Stress intensity factor coefficient for a lug loaded by pins with flats

Fig 10

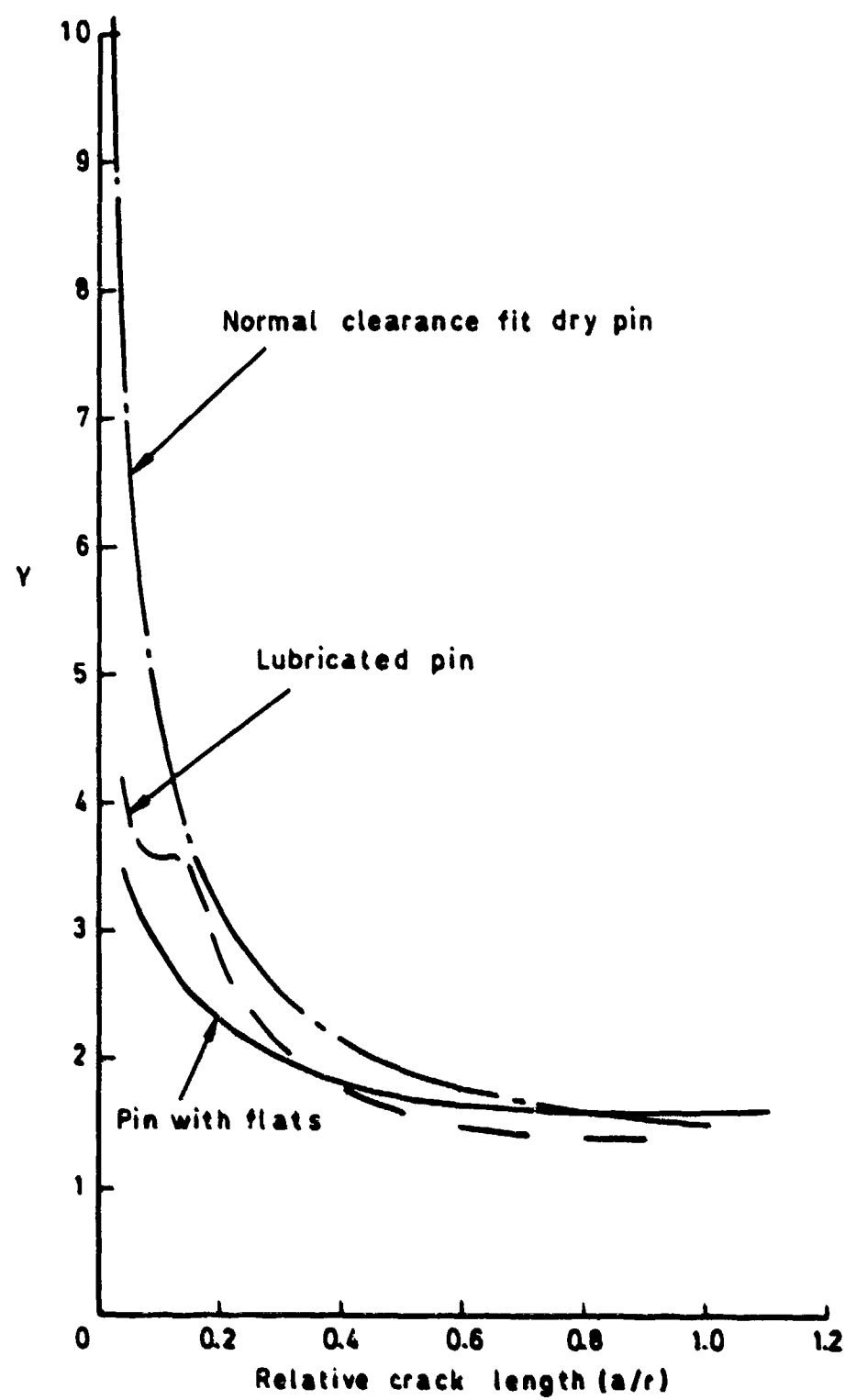


Fig 10 Comparison of experimentally derived stress intensity factor coefficients

Fig 11

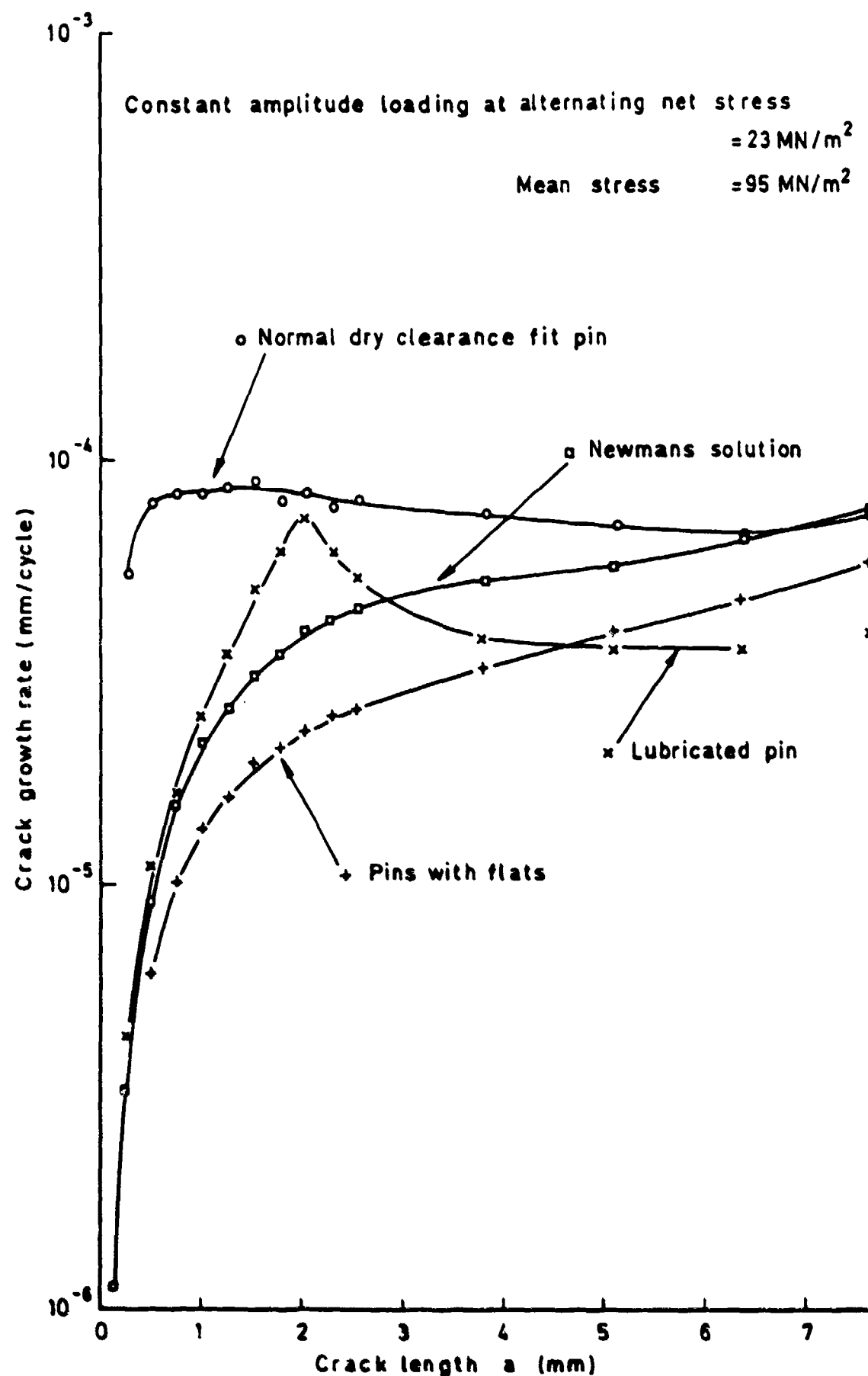


Fig 11 Effect of type and surface condition of pin on crack growth rate

Fig 12

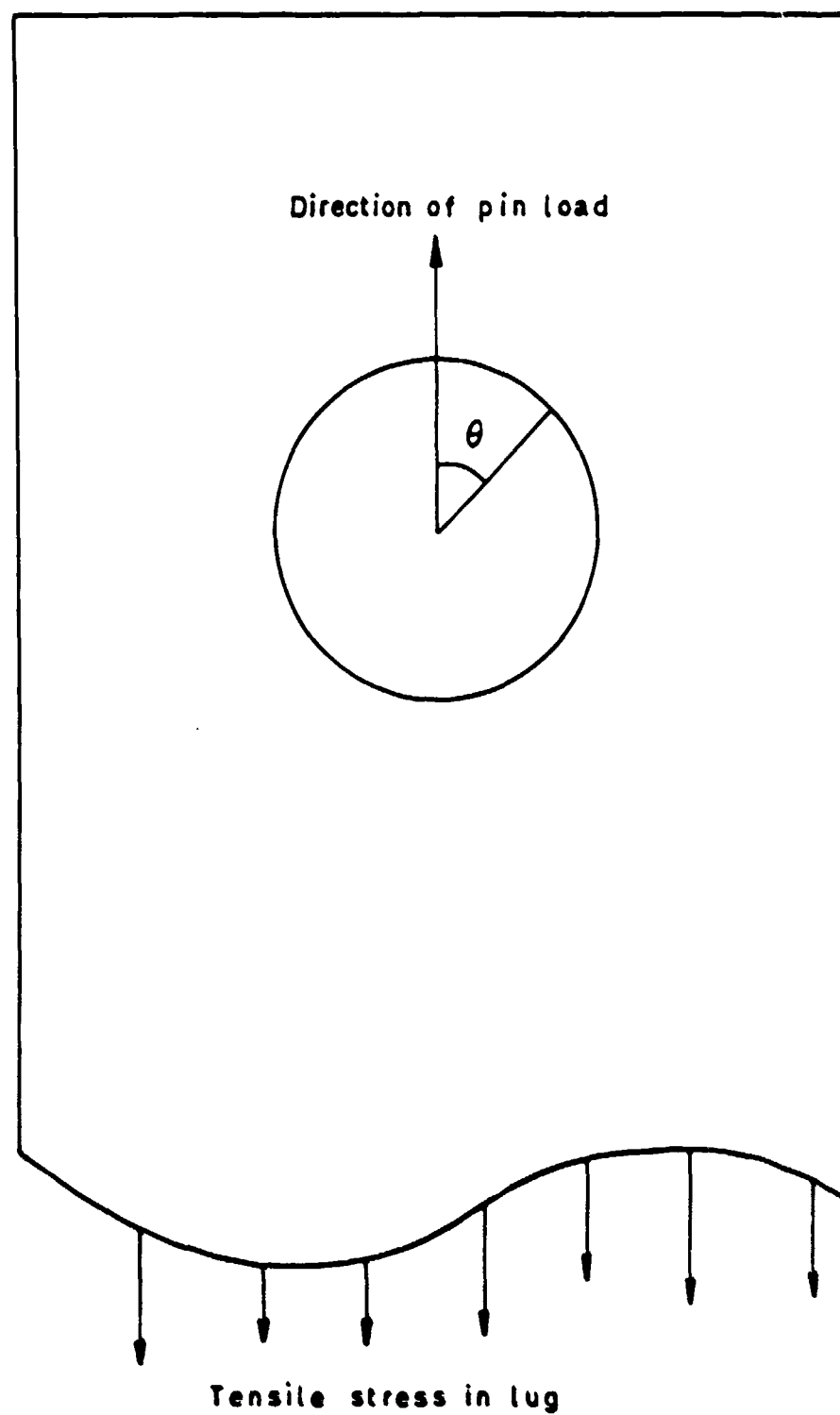
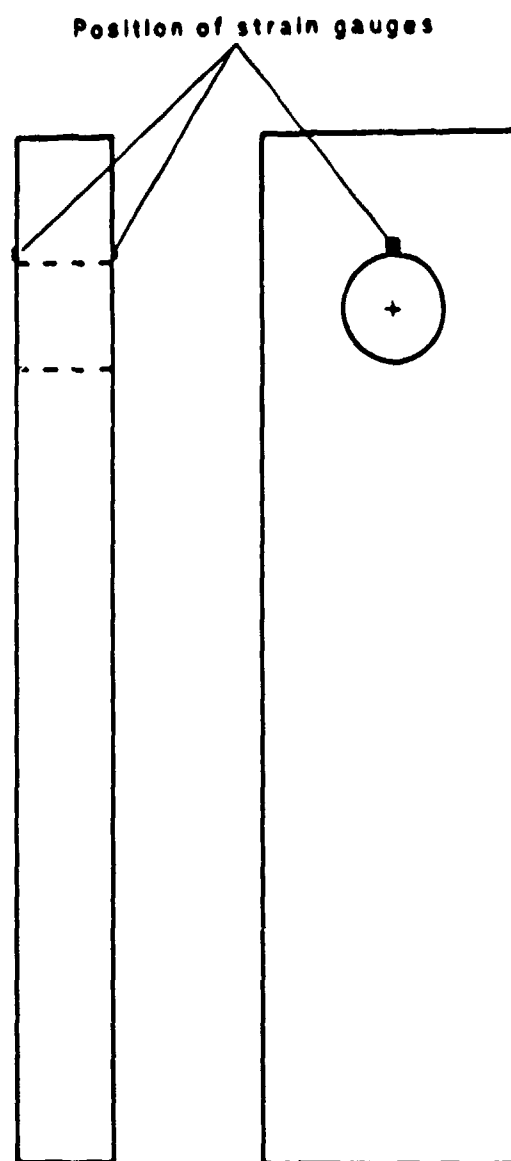


Fig 12 Definition of angle θ

Fig 13



All dimension as shown on Figure 1
Material - 7075 T7351
Loading pin - 594 steel

Fig 13 Specimen used to assess the effect of cycling on radial strain

Fig 14

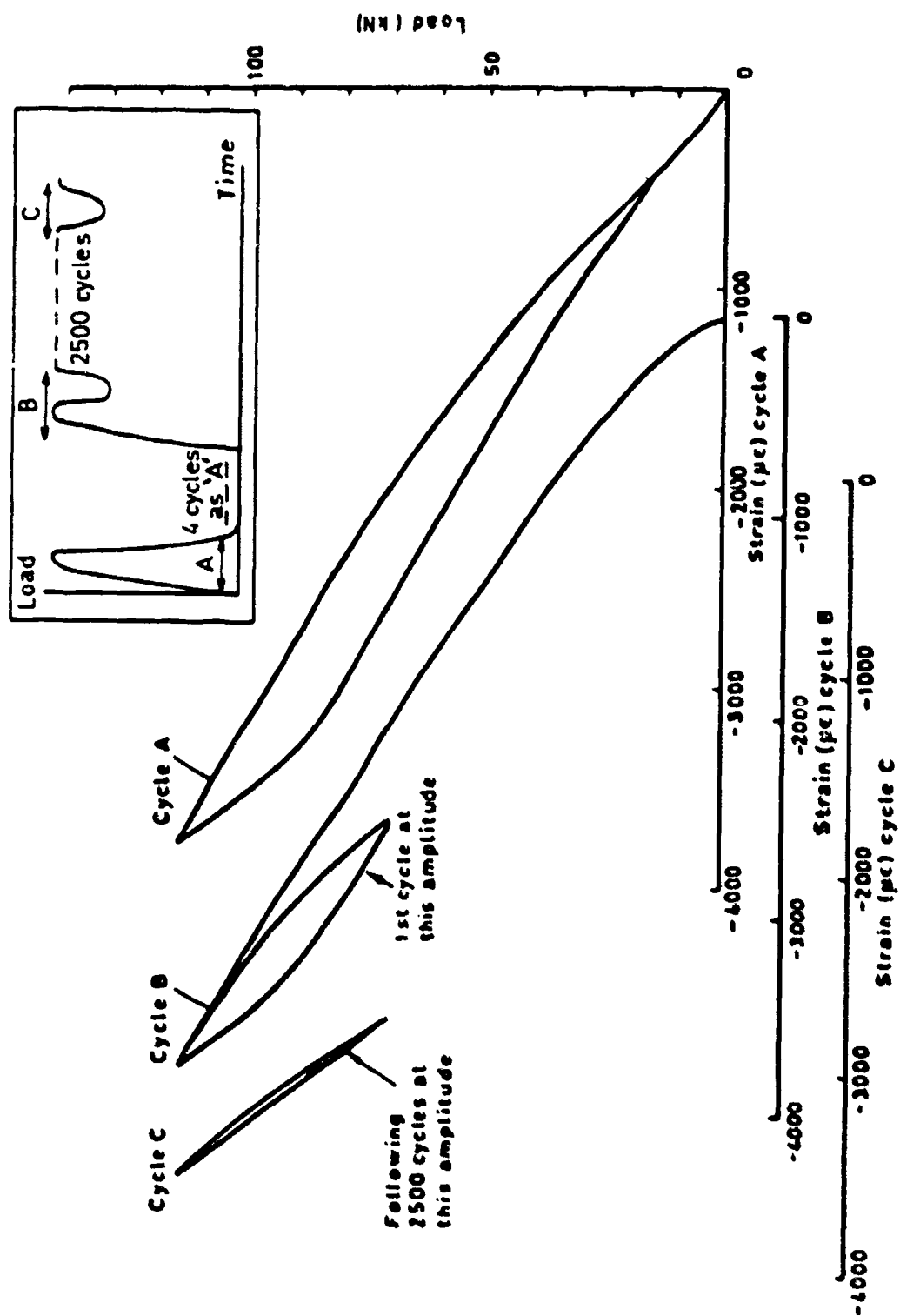


Fig 14 Strain-load history for cycles A, B and C at the top of the hole

Fig 15

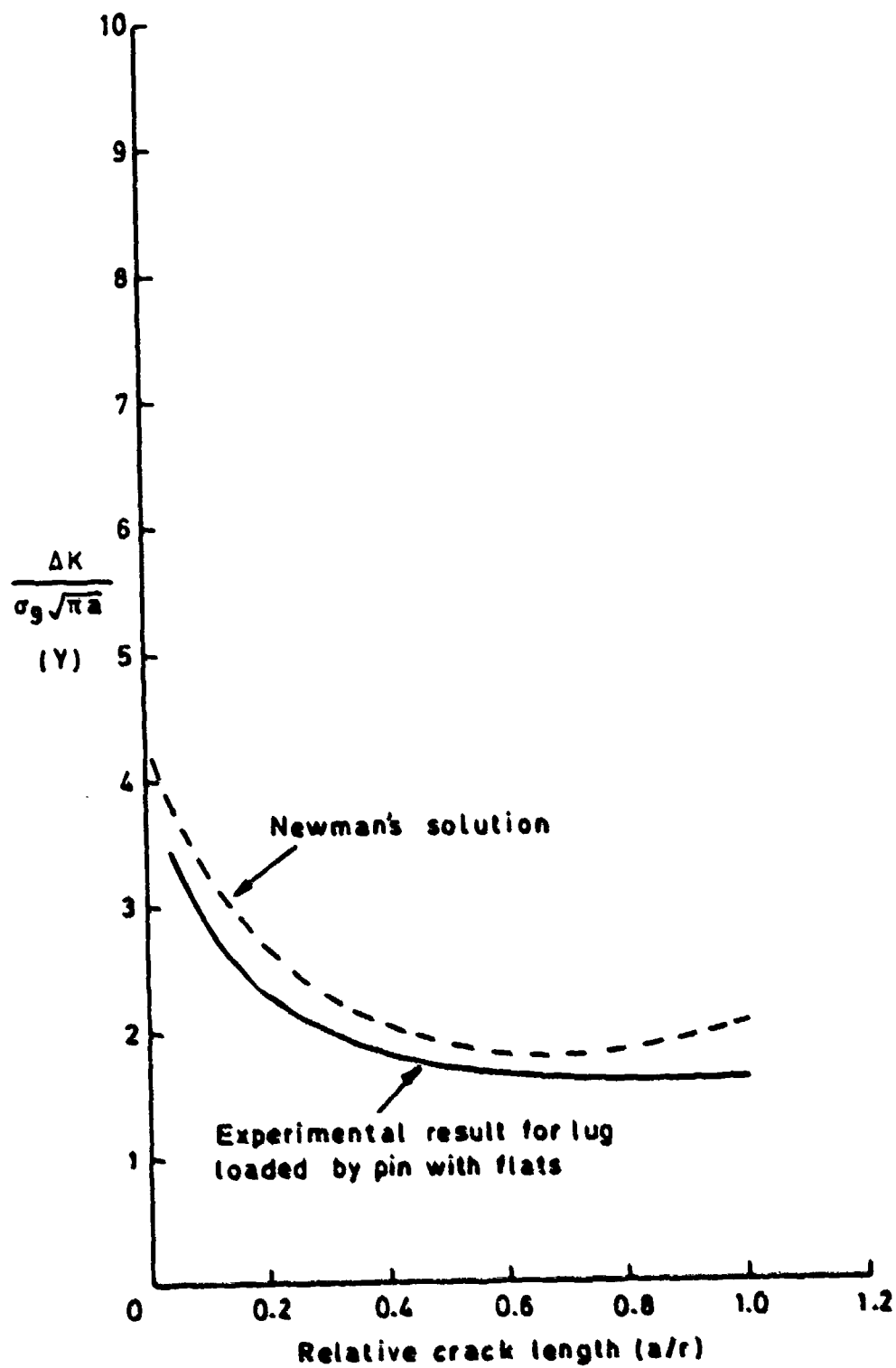


Fig 15 Newman's solution - the starting point of the prediction

Fig 16

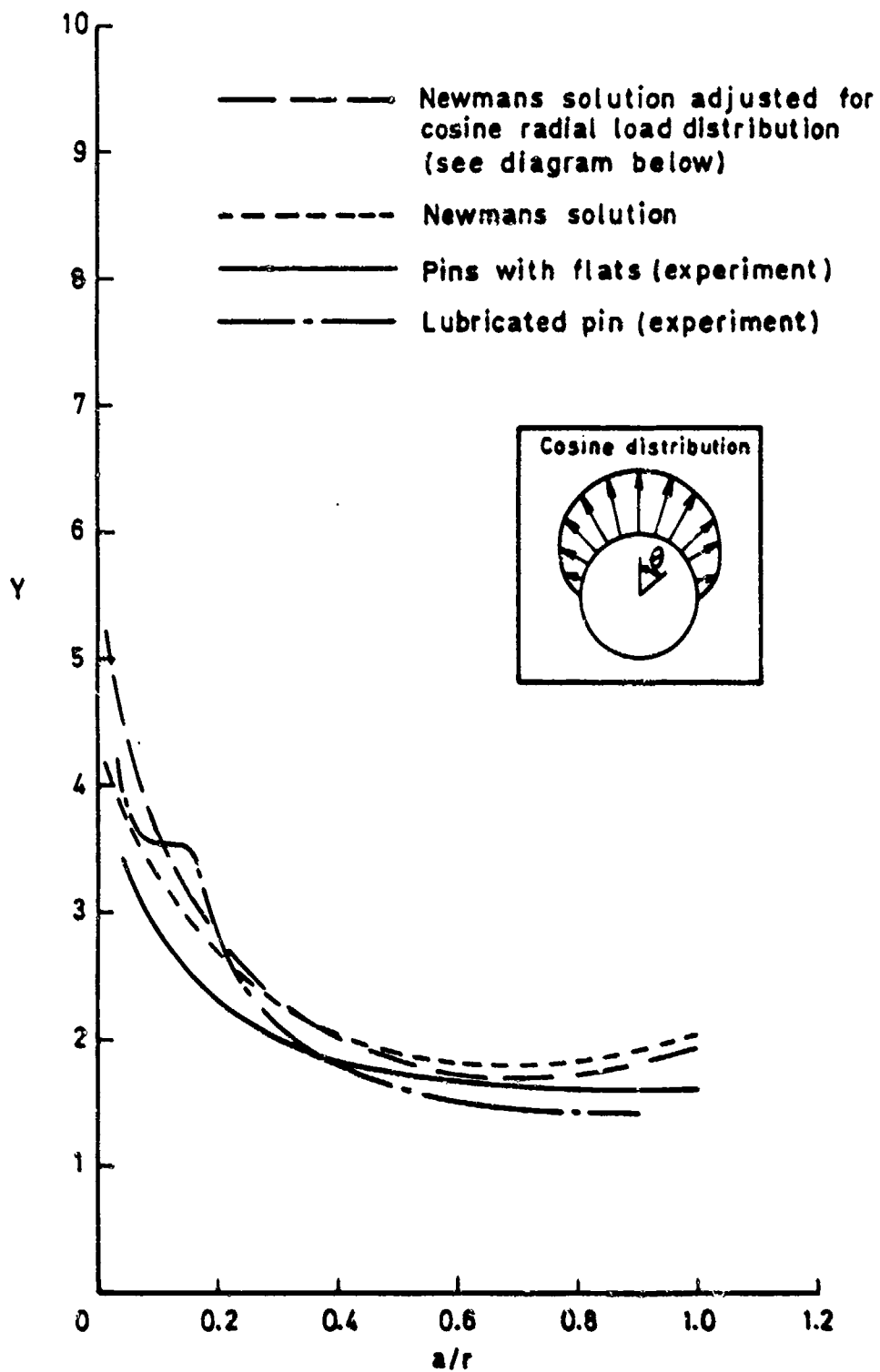


Fig 16 Effect of adjusting Newman's solution for a cosine radial pressure distribution

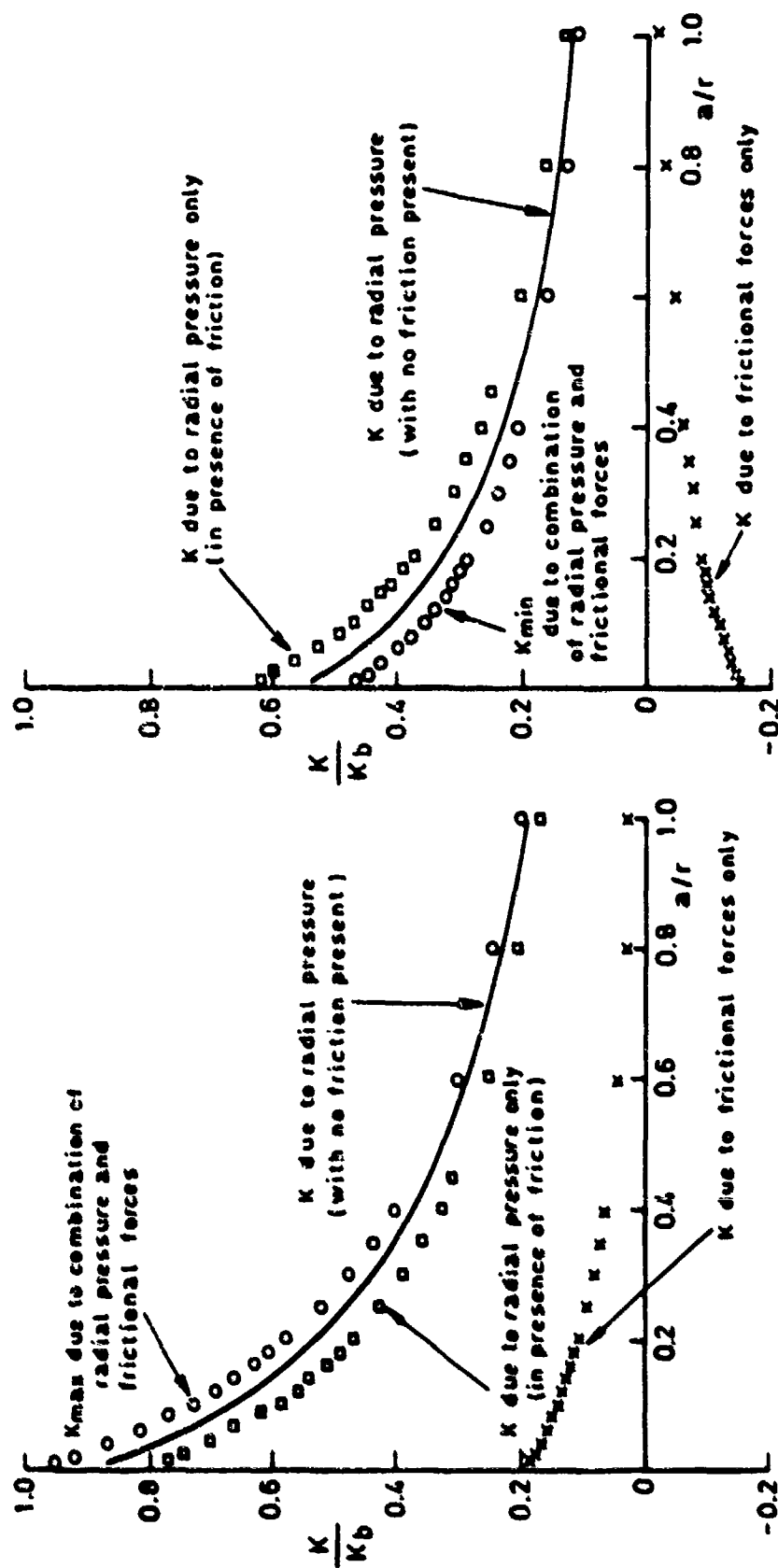


Fig 17a&b Calculation of K_{max} and K_{min} due to radial pressure and frictional forces for an infinite sheet

Fig 18

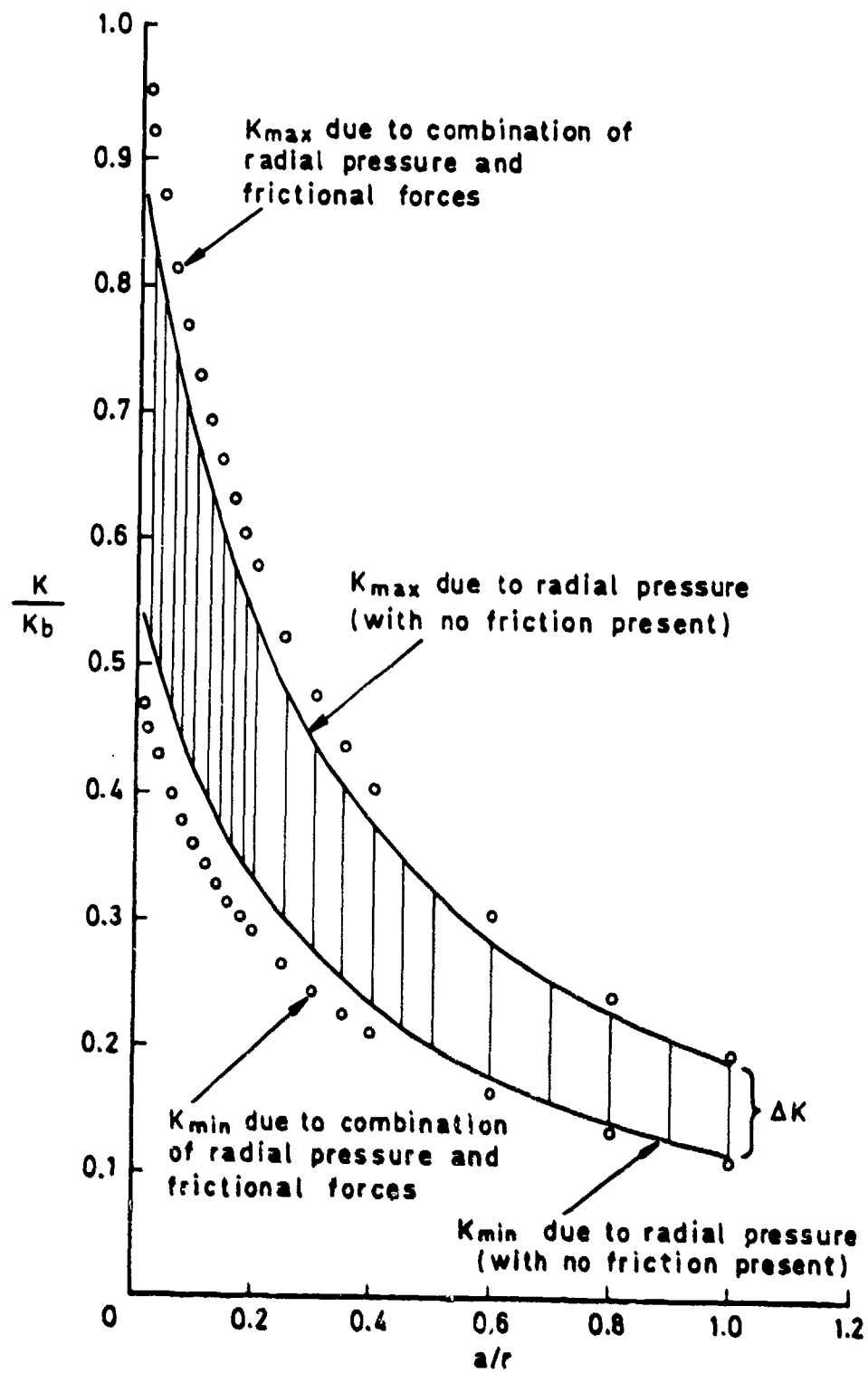


Fig 18 Increase in ΔK due to the presence of frictional forces

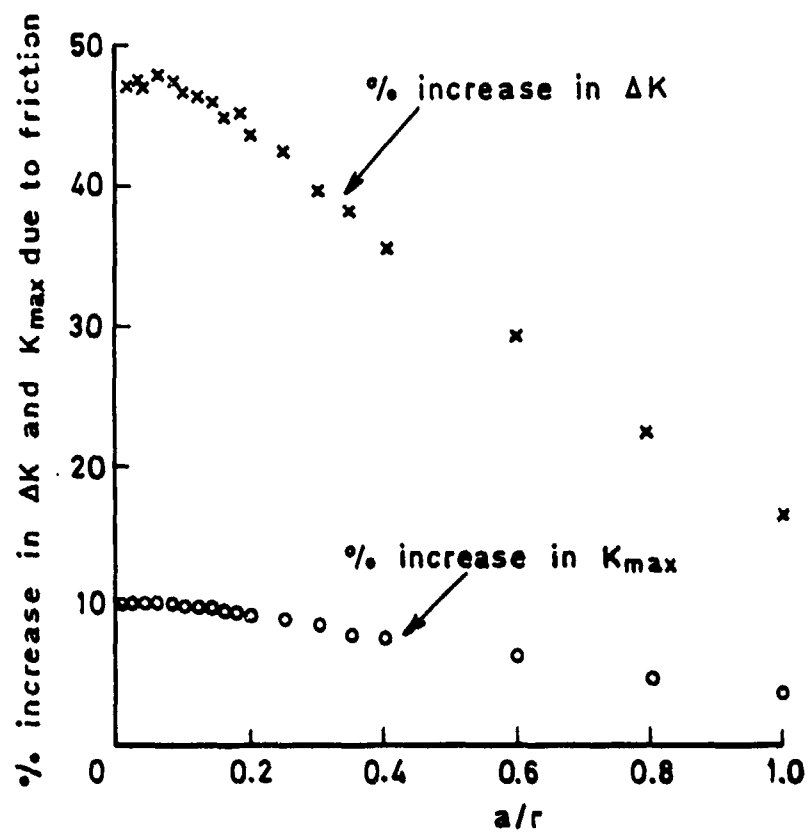


Fig 19 Percentage increase in ΔK and K_{max} due to the presence of frictional forces

Fig 20

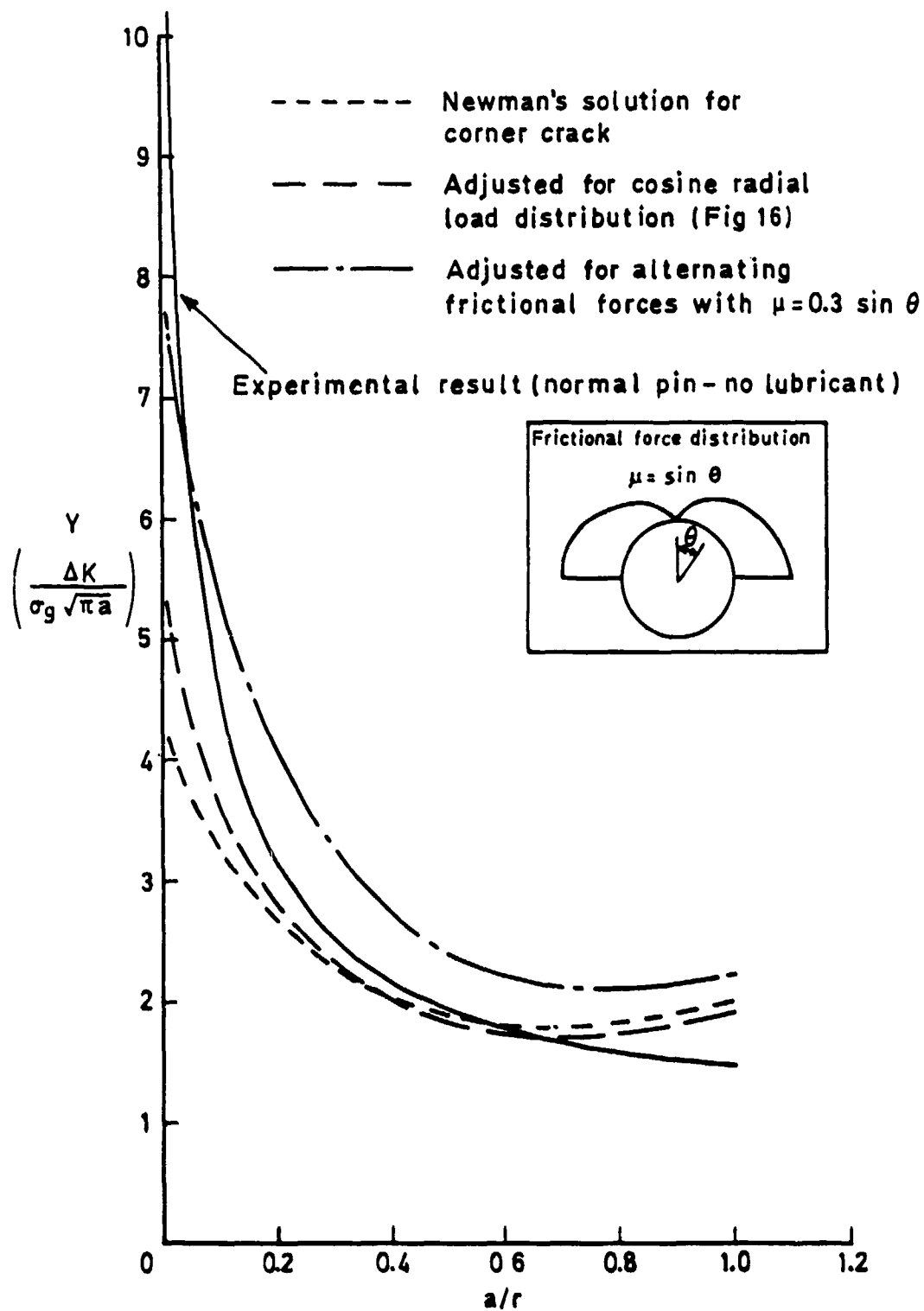


Fig 20 Effect of the inclusion of alternating frictional forces with $\mu = 0.3 \sin \theta$

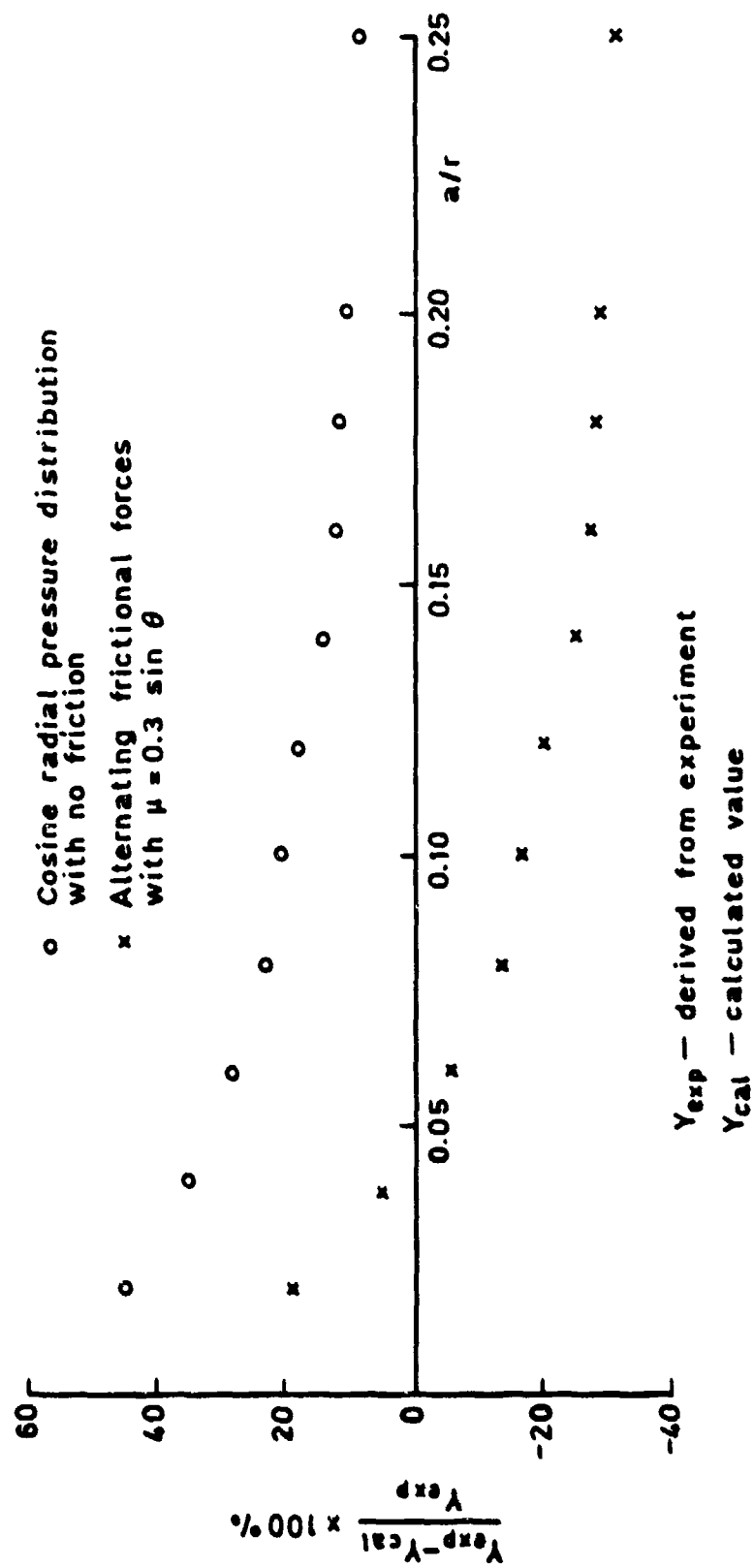


Fig 21 Comparison of errors in calculating Y with and without inclusion of frictional forces

Fig 22

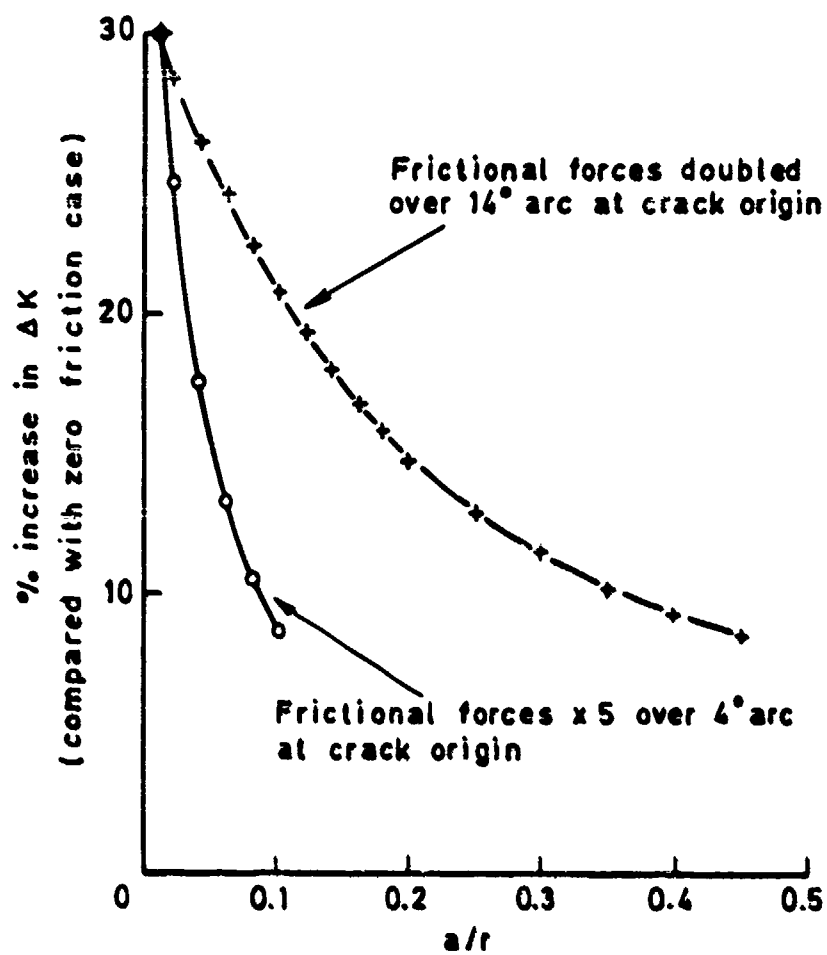
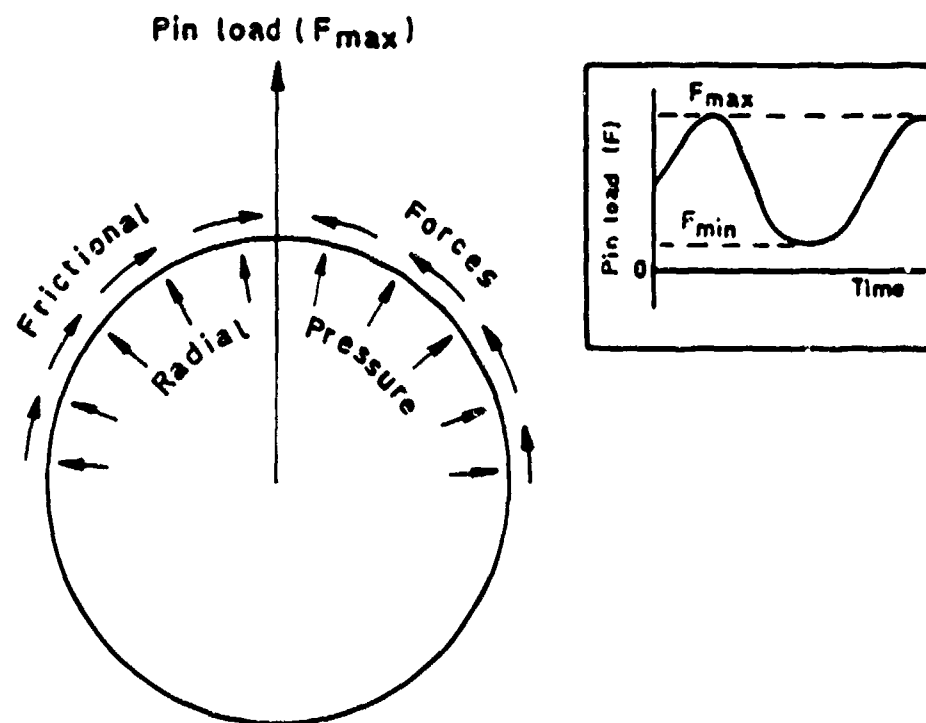


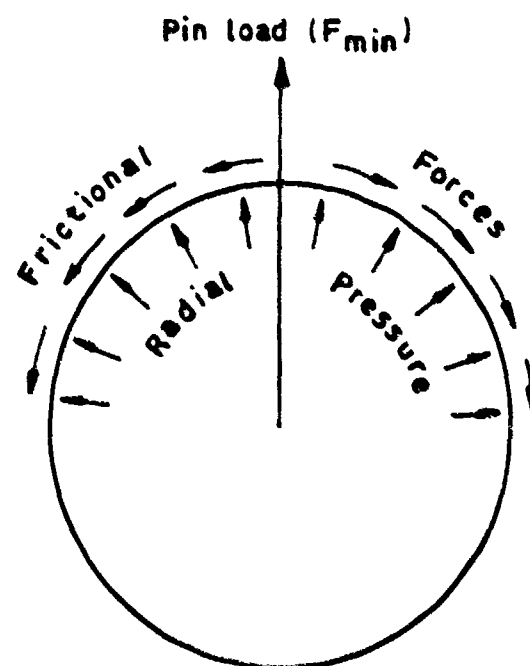
Fig 22 Effect of increasing frictional forces close to crack origin

UNLIMITED

Fig 23a&b



a) Forces acting on hole surface as pin load approaches maximum value in load cycle



b) Forces acting on hole surface as pin load approaches minimum value in load cycle

Fig 23a&b Schematic diagram of forces acting on hole surface during load cycling

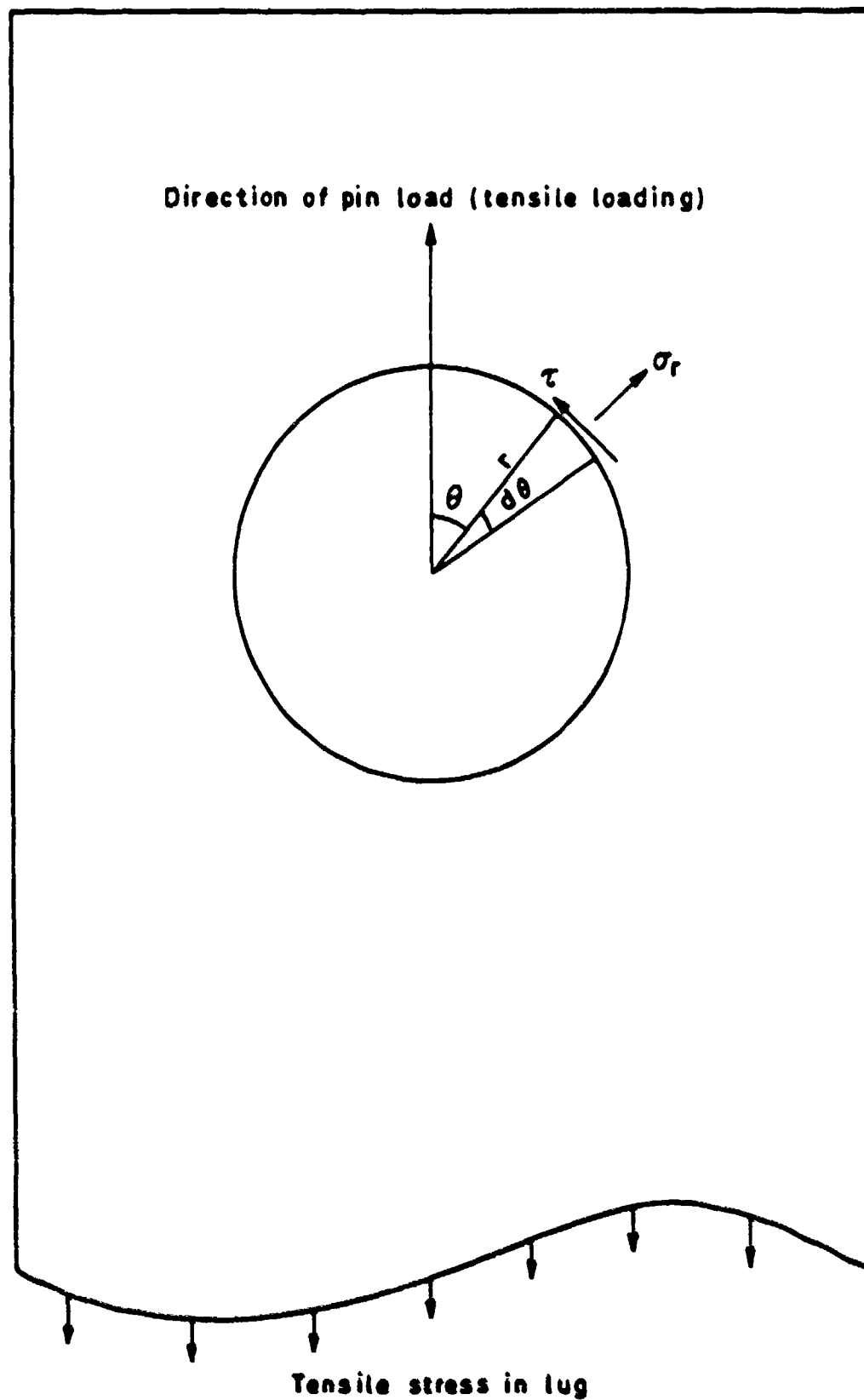


Fig 24 Consideration of forces acting on small element of hole surface

REPORT DOCUMENTATION PAGE

Overall security classification of this page

UNCLASSIFIED

UNLIMITED

As far as possible this page should contain only unclassified information. If it is necessary to enter classified information, the box above must be marked to indicate the classification, e.g. Restricted, Confidential or Secret.

1. DRIC Reference (to be added by DRIC)	2. Originator's Reference RAETR 84035	3. Agency Reference N/A	4. Report Security Classification/Marking UNCLASSIFIED		
5. DRIC Code for Originator 7673000W		6. Originator (Corporate Author) Name and Location Royal Aircraft Establishment, Farnborough, Hants, UK			
5a. Sponsoring Agency's Code N/A		6a. Sponsoring Agency (Contract Authority) Name and Location N/A			
7. Title The effect of frictional forces on fatigue crack growth in lugs					
7a. (For Translations) Title in Foreign Language					
7b. (For Conference Papers) Title, Place and Date of Conference					
8. Author 1. Surname, Initials Moon, J.E.	9a. Author 2	9b. Authors 3, 4		10. Date April 1984	Pages 48
				Refs. 17	
11. Contract Number N/A	12. Period N/A	13. Project		14. Other Reference Nos. Materials/ Structures 79	
15. Distribution statement (a) Controlled by - (b) Special limitations (if any) -					
16. Descriptors (Keywords) (Descriptors marked * are selected from TEST) Fatigue. Pinned lugs. Crack growth. Stress intensity factor. Fracture surface analysis. Fracture mechanics.					
17. Abstract In a previous Report crack propagation rate (da/dN) measurements were presented for a pin loaded lug. It was shown that da/dN of short cracks was much higher, by up to almost an order of magnitude, than predicted by available fracture mechanics solutions. It was proposed that this was due to the action of frictional forces between the pin and hole surface which are normally ignored in a fracture mechanics analysis, it being assumed that load is transferred by radial pressure alone. Further experiments have been conducted in which the frictional forces were reduced by lubricant and removed altogether from around the crack origin using pins with flats. It is found that both of these methods significantly reduce da/dN for short cracks. The inclusion of the action of frictional forces in a fracture mechanics analysis of a lug is shown to increase the predicted values of da/dN at short crack lengths. Closer agreement with experimental results is obtained if it is assumed that these forces build up more in the region of the crack origin and are thus effective for the important region of short crack lengths.					

1/0165